NPS ARCHIVE
1967
TOWLE, R.

THE MEASUREMENT OF THIN OIL FILMS UNDER DYNAMIC LOADING CONDITIONS, USING LIGHT AND X-RAY TECHNIQUES

ROBERT LELAND TOWLE

THE MEASUREMENT OF THIN OIL FILMS UNDER DYNAMIC LOADING CONDITIONS USING LIGHT AND X-RAY TECHNIQUES

by

Robert Leland Towle
Lieutenant, United States Navy
B.S., Naval Academy, 1960

Submitted in partial fulfillment of the
requirements for the degree of

MASTER OF SCIENCE IN MECHANICAL ENGINEERING

from the

NAVAL POSTGRADUATE SCHOOL
June 1967

ABSTRACT

This work attempted to study the behavior of thin oil films under dynamic loading conditions using light and x-ray techniques. This was done by passing light and x-ray beams between two cylindrical disks which suddenly squeezed oil films between them. The light technique presents a time variation of oil film thickness under sudden load conditions with good results. The x-ray technique attempted to measure counts from the x-ray beam during the very short time interval of minimum film thickness. Erratic and unreliable results from use of this technique indicate a different approach will have to be taken to measure thin oil films under dynamic loads.

LIBRARY
NAVAL POSTGRADUATE SCHOOL
MONTEREY, CALIF. 93940

TABLE OF CONTENTS

Section		Page
1.	Introduction	9
2.	Theoretical Considerations	12
3.	Test Apparatus	16
4.	Instrumentation	22
5.	Calibration Procedure	39
6.	Test Procedure	50
7.	Experimental Results	53
8.	Discussion of Results	63
9.	Conclusions and Recommendations	70
10.	Bibliography	72
Appendix I - Lubricant Specifications		75
Appendix II - Correlation of Load and Drop Angle		79
Appendix III - Absorption Data on Test Surfaces		85

LIST OF ILLUSTRATIONS

Figure		Page
1.	Test Apparatus	17
2.	Testing Surface	18
3.	Loading Device and X-ray System	19
4.	Schematic of Light and X-ray Systems	21
5.	Spectral Sensitivity of 5819 Photo-multiplier Tube	24
6.	Schematic of X-ray Tube	25
7.	Copper Radiation Spectrum	27
8.	Spectral Response of NaI.Tl Scintillation Counter Type 52245	29
9.	Schematic of Instrumentation	31
10.	Schematic of Single-Pulse Generator	34
11.	Schematic of Gate Circuit	35
12.	Instrumentation	36
13.	Instrumentation	38
14.	Calibration Arrangement	40
15.	Electrical Calibration Circuit	42
16.	Hypodermic Syringe for Filtering Oil	45
17.	Calibration Curve for Light System	46
18.	Calibration Curve for X-ray System	48
19.	Calibration Curve for X-ray System	49
20.	Overshoot of Light Signal	50
21.	Test At 50 RPM and 5.5 Degrees	54
22.	Test At 50 RPM and 10.25 Degrees	55
23.	Test at 100 RPM and 5.5 Degrees	56

24. Test At 100 RPM and 10.25 Degrees 57

25. Test At 150 RPM and 5.5 Degrees 58

26. Test At 150 RPM and 10.25 Degrees 59

27. Test At 200 RPM and 5.5 Degrees 60

28. Test At 200 RPM and 10.25 Degrees 61

A-1. Viscosity vs Temperature for 2110TH Oil 76

A-2. Viscosity vs Temperature for 2110TH Oil 77

ACKNOWLEDGEMENTS

I am very grateful to Professor E. K. Gatcombe for his advice, encouragement, and assistance during this investigation. The advice of Professor S. H. Kalmbach on the optical system and the assistance and loan of X-ray equipment by Professor J. R. Clark are gratefully appreciated. Thanks also go to the many people in the machine shop and Research Department who cheerfully assisted in building and instrumenting the test apparatus.

My very special appreciation goes to my wife Mary, daughter Suzanne, and Charlie Brown for their love, patience and understanding during this work.

1. Introduction

In the design of modern machinery, lubrication has come to play a vital role. Lubrication determines not only the performance characteristics, but also the reliability of machinery to operate. This is particularly true of gearing being designed for use in industry and military service. The trend has been and will undoubtedly continue to be towards higher load carrying capacities and higher speeds. With this apparent trend, it becomes vital that the problem of lubrication be well understood.

The problem of lubrication in gears, bearings, etc. is an old one and a significant amount of work has been done to study the behavior of lubricants in these applications. Various electrical methods have been applied to the measurement of thin oil films. El Sisi and Shawki [1] used an electrical conductivity technique with an additive in the lubricant to increase the electrical conductivity. MacConochie and Cameron [2] measured the voltage drop across thin oil films of loaded gear teeth. Their experimental results proved to be of the same order of magnitude compared with theoretical results. Shiflette [3] attempted to measure minimum oil film thickness in partial sleeve bearings by relating capacitance of the bearing and dielectric breakdown of the oil to film thickness. These methods have run into criticism for several reasons. First, precise rheological data on lubricants under high pressures is not available. Second, calibration data was obtained under unloaded conditions while the tests have been run up

to high load conditions. Elastic flattening of test surfaces therefore appears to alter the conditions under which electrical measurements are made.

Klorig [4] used a second basic technique of passing light through oil films. This work was carried on and refined with good results by Hydinger [5] . The one basic drawback to this system is the optical absorption of light by lubricants. There is also no data available as to the change in optical absorption of typical lubricants under pressure.

A third technique which shows considerable promise was developed by Sibley and Orcutt [6] . This is a direct x-ray transmission technique used to measure lubricant film thickness and shape of deformed bearing surfaces in rolling-contact lubrication. Using this method, they measured film thicknesses down to three microinches with an estimated accuracy of two microinches. The main feature of this technique is that the attenuation of x-rays in materials is an atomic phenomenon and is independent of such molecular phenomenon as viscosity.

The work done by Sibley and Orcutt was under steady load conditions using long counting times to determine x-ray transmission through the lubricants. The object of this investigation is to study the feasibility of measuring thin oil films under dynamic loading conditions using the x-ray technique. Since the light technique yielded good results for oil film thicknesses down to 500 microinches, simultaneous tests using both techniques will check the validity of data obtained from the x-ray technique. Valid results will permit

further investigation of thin oil films in the range of 20 to 50 microinches using this x-ray technique.

2. Theoretical Considerations

Lubrication has been widely studied for many years. As one would expect, many theories have been advanced to explain the effect of various parameters upon lubrication. Quite naturally, theory is only as good as its ability to withstand experimental investigation provided, of course, that all experimental errors can be identified and accounted for.

In studying lubrication in gears and rolling bearings, early theories used the Reynold's equation to explain dynamic lubrication. These theories, however, proposed film thicknesses that were so small, even under light loads, that they cast doubt on the very existence of lubrication in gears and rolling bearings. In recent years several new theories have been proposed which more closely agree with experimental results.

The two which appear to be most popular for critical examination with experimental results are those of Grubin [7] and Dowson and Higginson [8] . Both of these formulas assume an isothermal Newtonian lubricant and account for surface deformation and viscosity increase with pressure. These theoretical formulas take on the following form:

Grubin: $$\frac{h_o}{R} = 1.13\left(\frac{P'}{E'R}\right)^{-0.091}\left(\frac{\mu_o \gamma V}{R}\right)^{0.727}$$

Dowson and Higginson: $$\frac{h_o}{R} = 0.927\left(\frac{P'}{E'R}\right)^{-0.13}\left(\frac{\mu_o V}{E'R}\right)^{0.7}\left(\gamma E'\right)^{0.6}$$

Where h_o is the minimum film thickness, R is the relative

undeformed radius $\left(\frac{1}{R} = \frac{1}{R_1} + \frac{1}{R_2}\right)$, P' is the load per unit axial contact width, μ_o is the absolute viscosity at atmospheric conditions, V is the total rolling velocity $(V = V_1 + V_2)$, γ is the pressure-viscosity coefficient defined by the formula $\mu = \mu_o e^{\gamma P}$, and E' is a reduced Young's modulus of elasticity defined by the formula

$$\frac{1}{E'} = \frac{1 - \upsilon_1^2}{\pi E_1} + \frac{1 - \upsilon_2^2}{\pi E_2}$$

where υ_1 and υ_2 are Poisson's ratio and E_1 and E_2 are Young's modulus of elasticity for the rolling surfaces.

Both of these theoretical equations indicate several points worthy of mention. First, the rolling velocity at which the two surfaces operate is a dominant factor and for higher rotative speeds, greater film thicknesses would be expected. Secondly, viscosity of lubricants under pressure increases and thereby increases the film thicknesses. Thirdly, the loads placed upon the contact areas play less of a role and tend to decrease the minimum film thickness as the load increases. One last point should be made that neither of these theories takes into account the effect of temperature of the lubricant in the region of contact, surface roughness of the mating surfaces, or compressibility of the lubricant.

Sibley, Bell, Kannel and Allen [9] found their experimental results to fall below those predicted by the theory

of Grubin and Dowson and Higginson. Their results, obtained by an x-ray technique, conform to the following equation:

$$\frac{h_o}{R} = 0.057 \left(\frac{P'}{E'R}\right)^{-0.36} \left(\frac{\mu_o \gamma V}{R}\right)^{0.73}$$

Their basic proposal to account for this difference is that the lubricants actually behave in a non-Newtonian manner. The theory proposed by Ree and Eyring [10] accounts for non-Newtonian behavior of lubricants.

A Newtonian lubricant is described by the relation between shear stress τ, and shear rate $\dot{s}$

$$\tau = \mu \dot{s}$$

where μ is lubricant viscosity, defined to be

$$\mu = \mu_o e^{\gamma P}$$

In the Ree-Eyring theory the relation between shear stress and shear rate takes on the form

$$\tau = \frac{X}{\alpha} \operatorname{SINH}^{-1}(\beta \dot{s})$$

where α is a constant and

$$X = X_o e^{\gamma_1 P}$$
$$\beta = \beta_o e^{\gamma_2 P}$$

with X_o and β_o being defined as constants for a particular lubricant at a constant temperature.

The basic result of this theory is that at low shear rates, lubricants will behave in a nearly Newtonian manner, but at high shear rates the shear stress develops at a slower rate. The end result is that non-Newtonian theory

predicts film thicknesses which are lower than those predicted for Newtonian theory.

The preceding discussion has not attempted to cover all theories, but rather to point out some of the dominant factors to be considered in hydrodynamic lubrication.

3. Test Apparatus

The test unit used for this investigation was basically the same unit used by Hydinger [5], modified as necessary to be used with an x-ray machine. The complete test unit, shown in Figure 1, consists of a rotating lower cylindrical disk and an upper cylindrical disk mounted in a pendulum arm.

The actual test surface shown in Figure 2 consists of a one-half inch wide by six inch diameter face. It is constructed of AlSl 8620 steel, case carburized to 1/16 inch with a hardness of 50-60 Rockwell C. The surface finish is 10 microinches center line average. The shaft is mounted on precision ground tapered roller bearings and has provision for adjusting the axial and radial clearance of the bearings by means of a clearance adjusting plate. The shaft was coupled to a hydraulic transmission and constant speed 1800 RPM A-C motor. With the hydraulic transmission, speed of the shaft could be varied in either direction. All connections were made with flexible couplings to minimize vibration of the test shaft. To measure shaft speed, a tachometer was geared directly to the shaft. Speed was also checked using a hand tachometer.

The dynamic loading device shown in Figure 3 was designed as a compound pendulum. By designing the pendulum so that the point of impact and center of percussion coincide, reactions at the pivot point are eliminated. The wheel held in the pendulum for sudden loading of the oil films is four

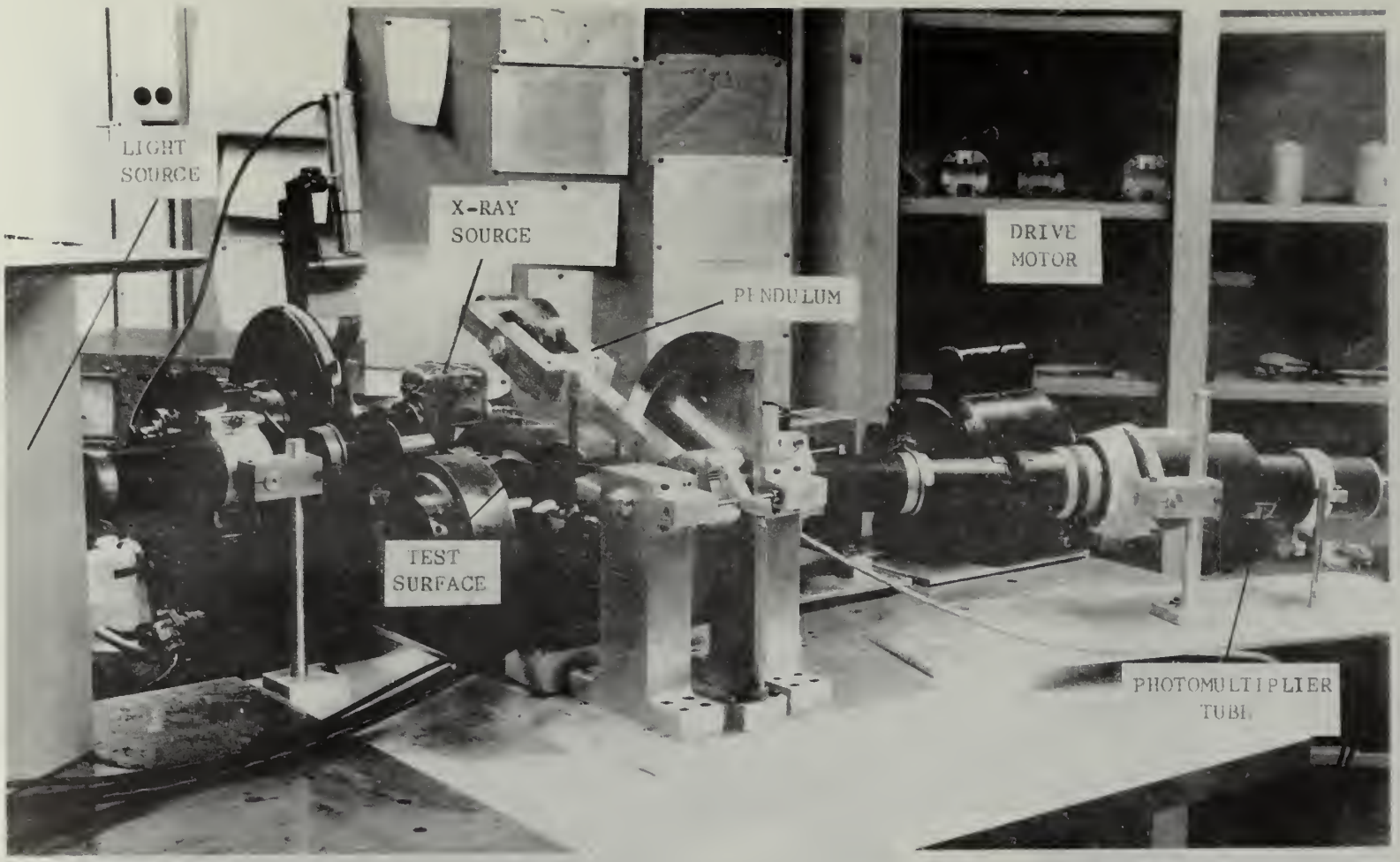

FIGURE 1. TEST APPARATUS

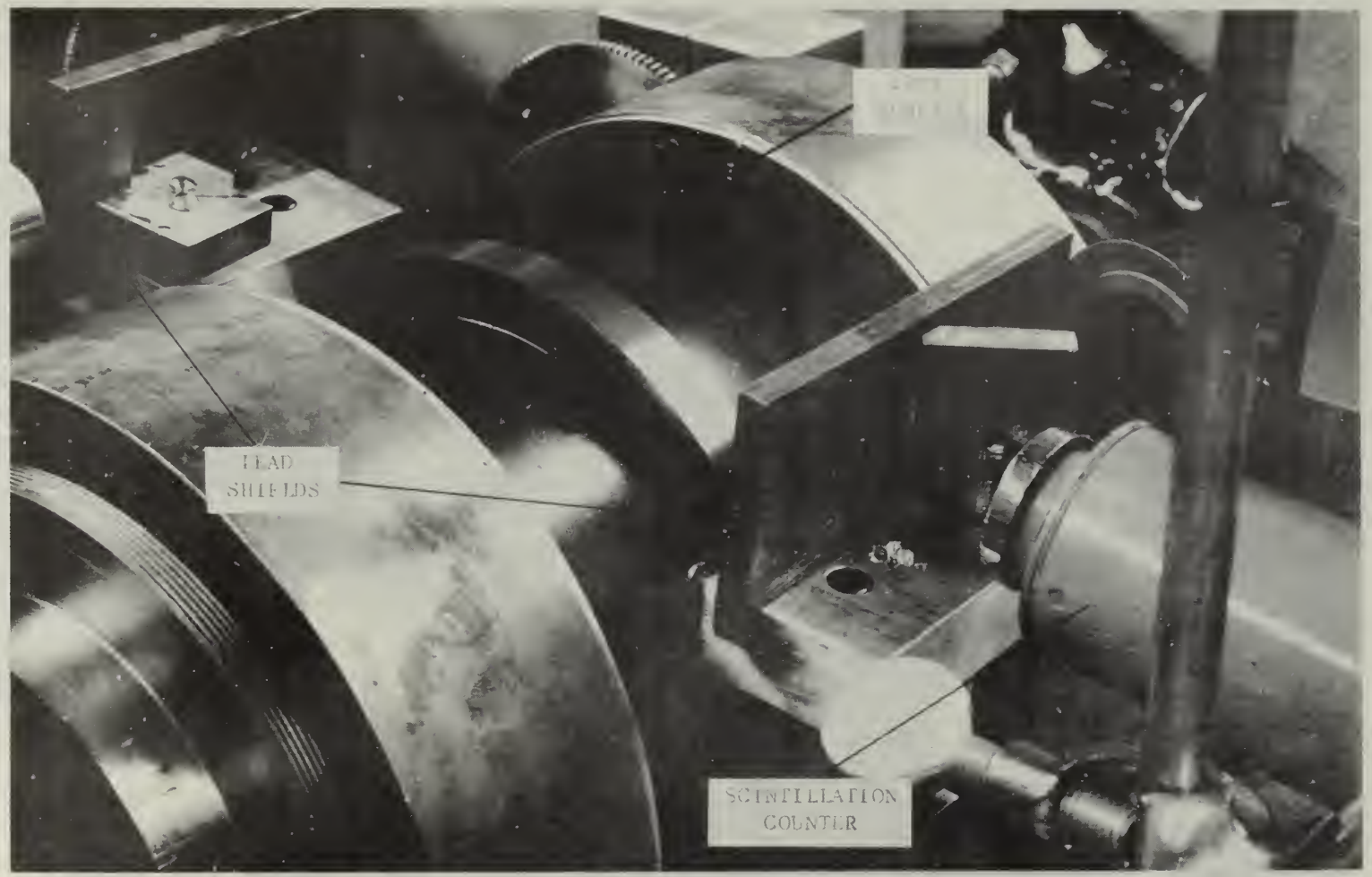

FIGURE 2. TESTING SURFACE

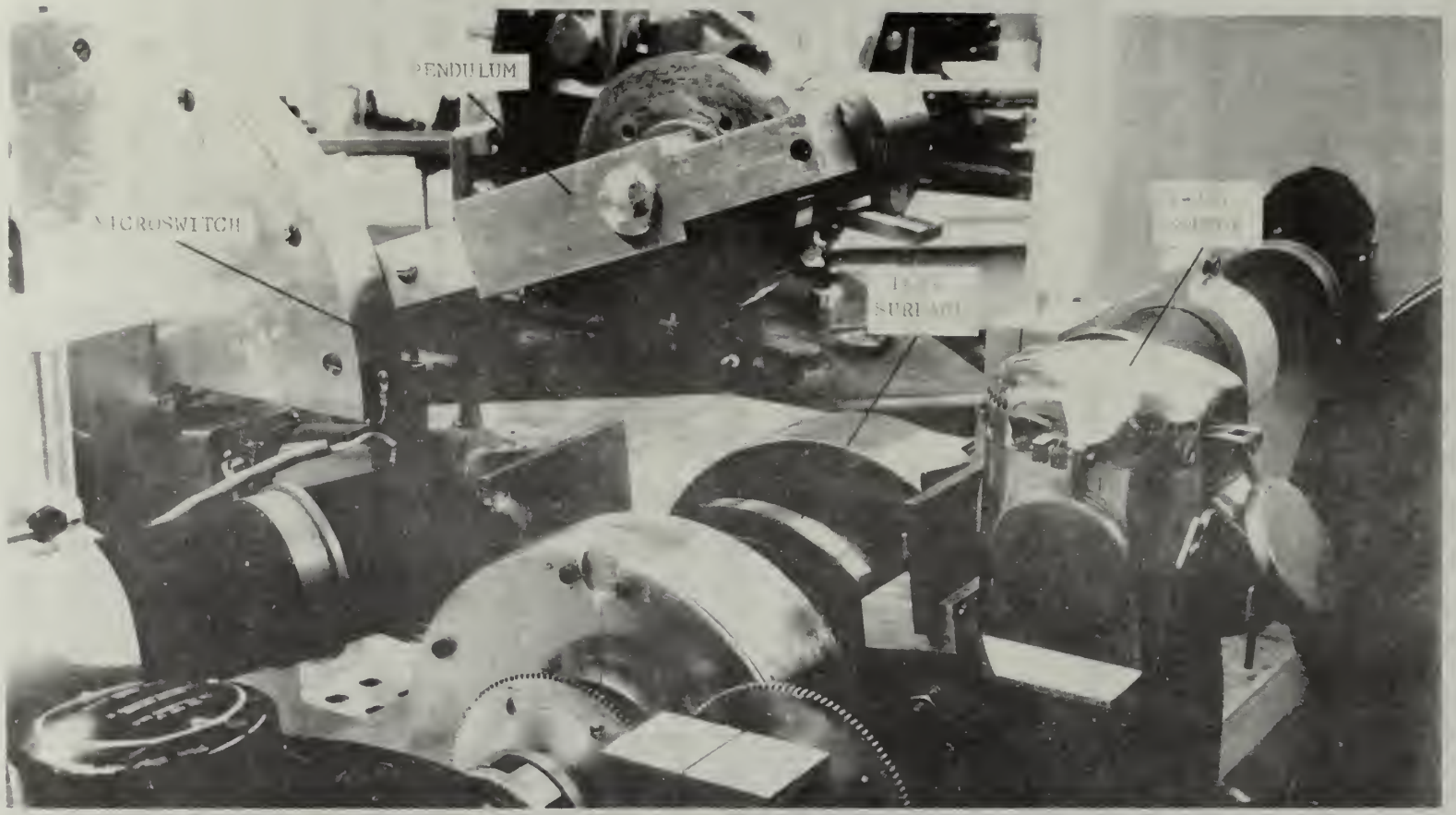

FIGURE 3. [illegible] DEVICE AND X-RAY SYSTEM

inches in diameter, and has a face width of one-half inch. It is made of AlSl 8620 steel with a surface finish of 10 microinches center line average. It is also case carburized to 1/16 inch with a hardness of 50-60 Rockwell C.

The pendulum design is such that the weight of the pendulum when released from heights provided sufficient dynamic loads on the oil films. A rachet was built into the hub of the pendulum to position and hold the pendulum until the test is ready. In order to insure parallelism between the two test surfaces, a ball and socket arrangement was used at the pivot point of the pendulum. Parallelism between the test surfaces was actually checked by seeing if the clean test surfaces, when together, completely cut off the light and x-ray signals. Lateral alignment of the pendulum was made by two adjusting nuts in the pendulum supports.

The whole test assembly was mounted on a 1 and 1/4 inch thick aluminum plate which was supported by five legs. To minimize vibration, the whole table assembly was mounted on one-half inch thick composition rubber and bolted to the deck. As a further attempt to minimize vibration, the A-C motor and hydraulic transmission were mounted on rubber before being bolted to the base plate.

As a safety precaution in working with x-rays, two 1/4 inch thick lead shields were placed in the path of the x-ray beam. One was placed in front of the test surface and the other behind the test surface. Both shields had a 1/16 x 1/2 inch slit for passage of a small portion of the beam to and from the test surface.

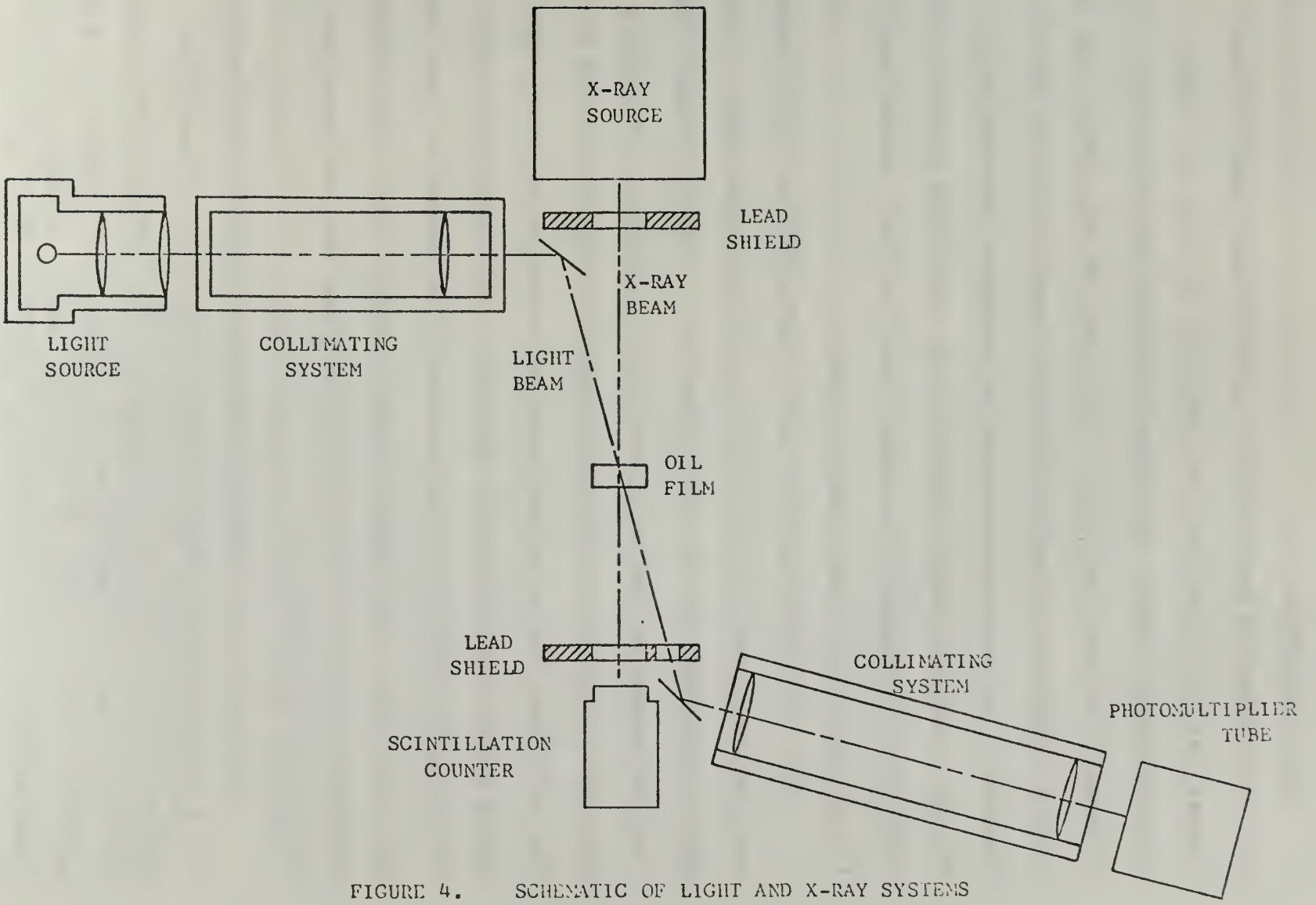

FIGURE 4. SCHEMATIC OF LIGHT AND X-RAY SYSTEMS

4. Instrumentation

Two separate and distinct methods were used in this investigation to measure the behavior of thin oil films under dynamic loads. The first of these was the sight system developed by Hydinger [5] . Since one of the basic aims of this investigation was to check the results of the two systems, the basic system used by Hydinger was unaltered. However, several basic modifications had to be made to the equipment arrangement in order that the light system would fit properly with the x-ray equipment.

The first consideration which affected the light system was consideration of the intensity of the x-ray beam. Radiation intensity from a point source is inversely proportional to the square of the distance from the source. Therefore, in order to obtain maximum intensity of the x-ray beam through the oil film, the test surfaces had to be as close to the x-ray source as physically possible. This physical limitation led to the relocating of the light source on one side and reflecting the light through the oil film. The reflecting surfaces used were .050 inch thick glass with an aluminum coating on one side.

The use of reflectors was another problem which resulted in a slight modification of the light path. The original design was for both the light and x-ray beams to travel along coincident paths through the oil film. This placed the glass reflectors in the path of the x-ray beam. However, since the glass attenuated too much of the x-ray and also suffered radiation damage within a short time period, the reflectors

had to be moved out of the path of the x-ray beam. The final arrangement used during the testing is shown in Figure 4.

Another factor which affected the physical arrangement of the system was the fact that the x-ray beam is slanted downward at a six degree angle from the horizontal. This required a modification of the pendulum arrangement so that the point of impact of the two disks was six degrees from the vertical. Due to the location of the photomultiplier tube, the collimating system and photomultiplier tube had to slope at a slight angle from the horizontal.

All the above-mentioned problems were a result of physical considerations. The end result of the modification was a light system basically the same as that used by Hydinger.

Due to the great detail with which all aspects of the light system were described by Hydinger, only a brief description of the basic components will be made. The light source used was a microscope illuminator with a ribbon filament, type SR-8, rated at six volts and 18 amperes. The power was supplied by two wet cell batteries of 175 amperehours capacity. This combination of light source and power supply provided a stable light signal free from ripple.

The detection device used for the light system was a packaged commercial unit comprised basically of a 5819 photomultiplier tube. This is a 10 stage, head-on type high vacuum tube having a spectral response curve as shown in Figure 5 . Maximum response occurs at 4000 ± 500 angstroms

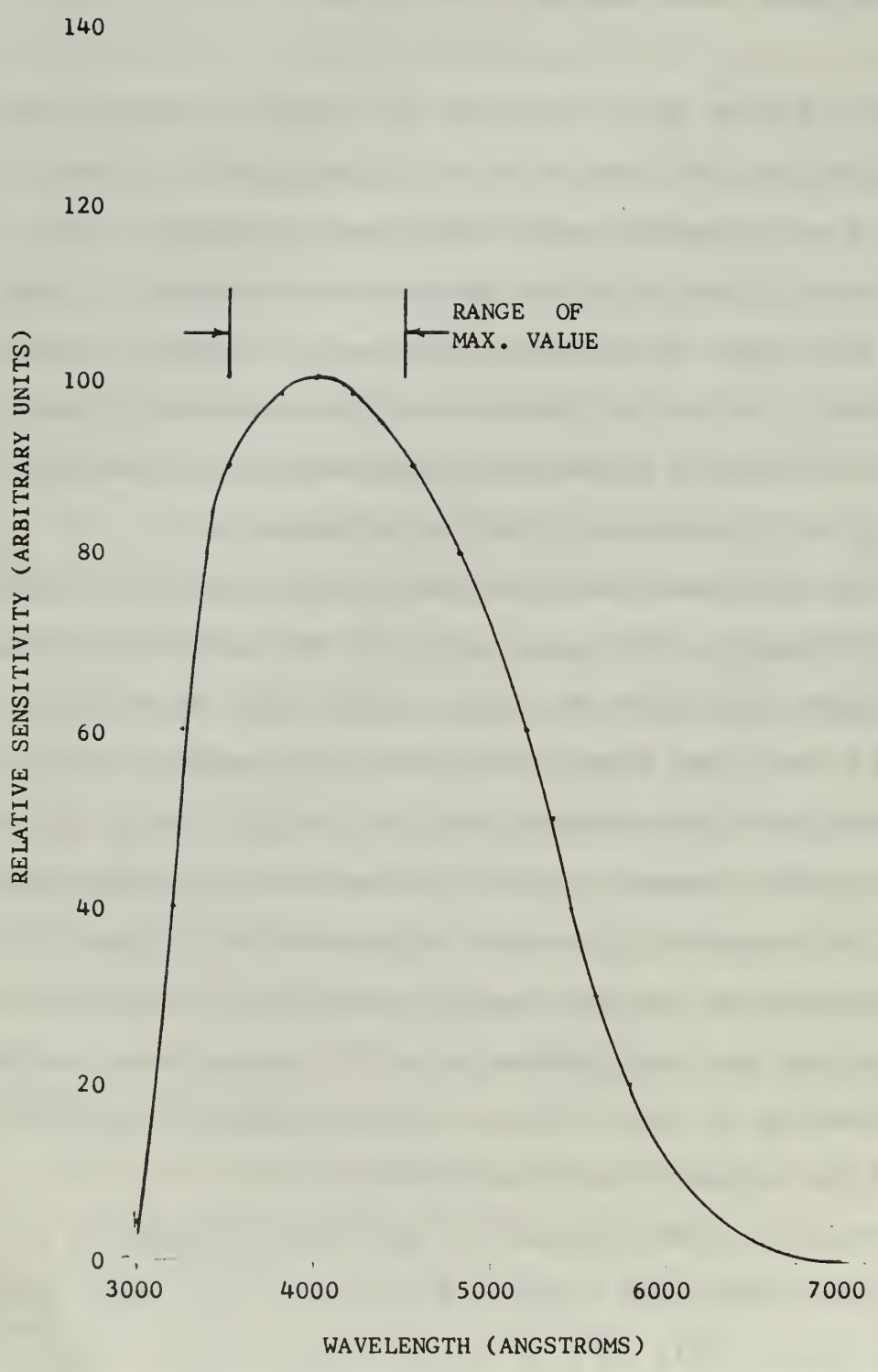

FIGURE 5. SPECTRAL SENSITIVITY OF 5819 PHOTOMULTIPLIER TUBE

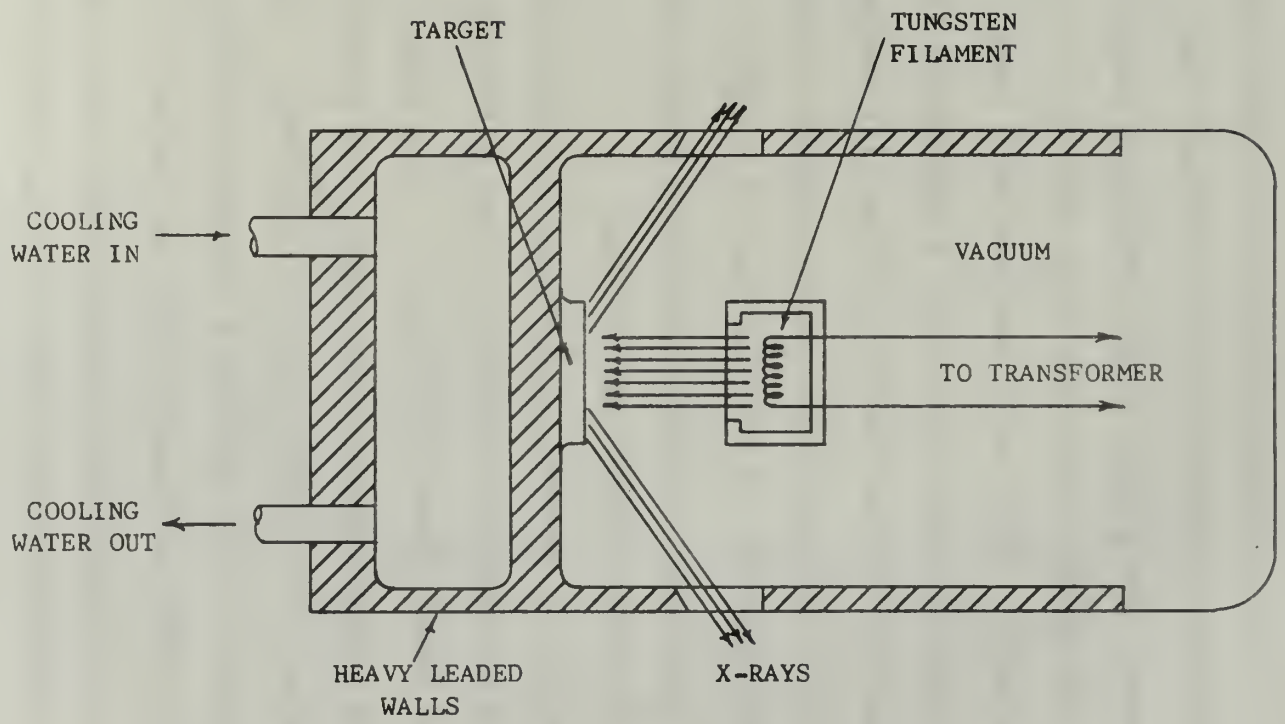

FIGURE 6. SCHEMATIC OF X-RAY TUBE

indicating a high sensitivity to blue light and negligible sensitivity to red radiation. One of the key advantages of this photomultiplier tube is its extremely high gain of approximately 500,000 when operated at a supply voltage of 1000 volts. This advantage imposed the requirement, however, that all tests be conducted under darkened room conditions in order to reduce the signal from extraneous sources.

The x-ray system centered about the use of an x-ray diffraction unit. This unit consists of a stable, shockproof full-wave rectified generator with a centrally mounted heavy leaded bronze x-ray tube housing. The high voltage generator power supply is end grounded and is capable of delivering up to 50 milliamperes at voltages up to 60 KVP. It is provided with convenient stepless controls which allow close adjustment of tube voltage and current.

The source of x-rays is a commercial high-vacuum x-ray tube mounted in the tube housing of the diffraction unit. This type of tube, shown in Figure 6, is a highly convenient and flexible x-ray source. The x-rays are generated from a target metal which is bombarded by electrons. The electrons in turn are excited by heating a tungsten filament. The rate at which the electrons strike the target is controlled by the tube current and the energy with which the electrons strike is controlled by the tube voltage. This then makes it possible to vary the intensity and wavelength of the x-ray beam independently. The target tube selected for this investigation was Copper operated at 50 KVP and 35 MA. While

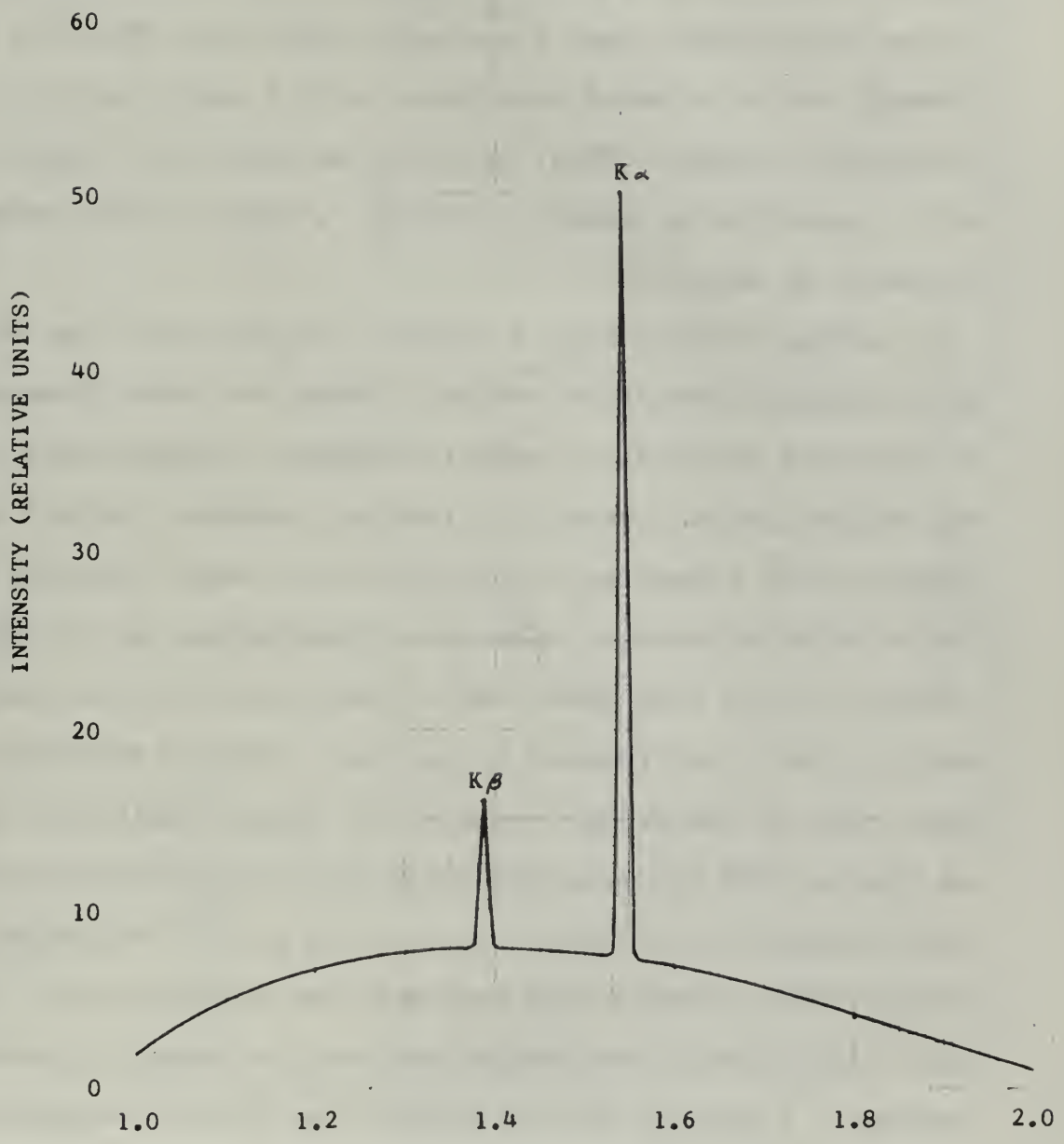

FIGURE 7. COPPER RADIATION SPECTRUM

Sibley and Orcutt used a filtered Molybdenum source, the uncertainty of the expected results in this work tipped the scales in favor of a source having a higher intensity since it was anticipated that fluorescent radiation from the surfaces framing the slit would contribute only a small amount to the radiation counted. Thus, by using an unfiltered Copper source with a spectrum as shown in Figure 7, higher count rates would normally be expected.

Having settled upon a source, the next step was selection of a suitable detection device. There are three general types of counters available: geiger counters, proportional counters, and scintillation counters. Dowling, Hendee, Kohler, and Parrish [11] presented a good review of these counters and their relative merits. The main disadvantage of the Geiger counter is its long dead time - that period of time during which it will not respond to another electron discharge. The dead time of the Geiger counter for Copper radiation can be as high as 270 microseconds resulting in appreciable deviation from linearity for count rates as low as 500 counts/sec. The Proportional counter does not run into this problem. The dead time between two counts need only be about 0.2 microseconds. Linearity of the counter can then be maintained up to count rates of one million counts per second. The Proportional counter does however have the serious disadvantage of low counting efficiency.

The Scintillation counter has characteristics similar to the Proportional counter. First, it has an extremely

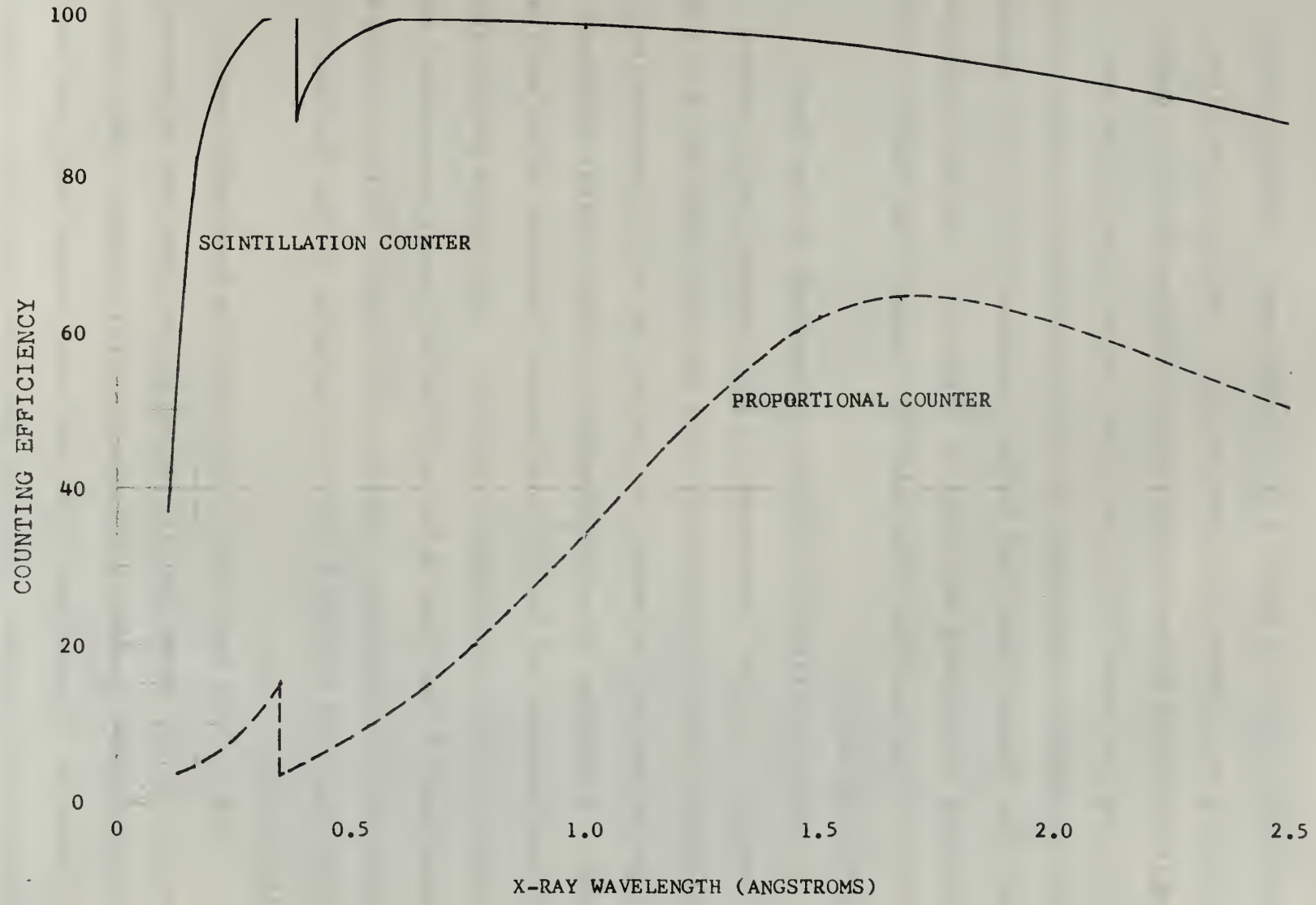

FIGURE 8. SPECTRAL RESPONSE OF NAI.Tl SCINTILLATION COUNTER TYPE 52245

short dead time of about 0.2 microseconds, ensuring linear counting up to very high intensities. Second, its pulse amplitudes are proportional to the quantum energy, thereby offering the possibility of pulse height discrimination. The outstanding advantage of the Scintillation counter over both the Proportional and Geiger counters is its high quantum counting efficiency as shown in Figure 8. For this combination of reasons, the Scintillation counter was chosen as the detection device.

The Scintillation counter is composed of two basic elements: a flat fluorescent single crystal and a photomultiplier tube. The crystal was NaI.Tl mounted in a light tight holder and attached to the end of a 6291 photomultiplier tube. A quantum of x-ray absorbed by the crystal produces a photo-electron and one or more Auger electrons which activate a number of the fluorescent centers. The Sodium Iodide crystal contained 1% Thallium which acts as a fluorescent center when energized by electrons. These centers emit visible photons which are then directed onto the cathode of the photomultiplier tube.

Due to the fact that the crystal is extremely hygroscopic, it is hermetically sealed in an aluminum holder which is completely opaque to external visible light. This makes it possible to use the light and x-ray techniques together without interference. During operation, the anode voltage of the photomultiplier tube was set at 800 volts. Background counts due to cosmic radiation and photo-multiplier noise

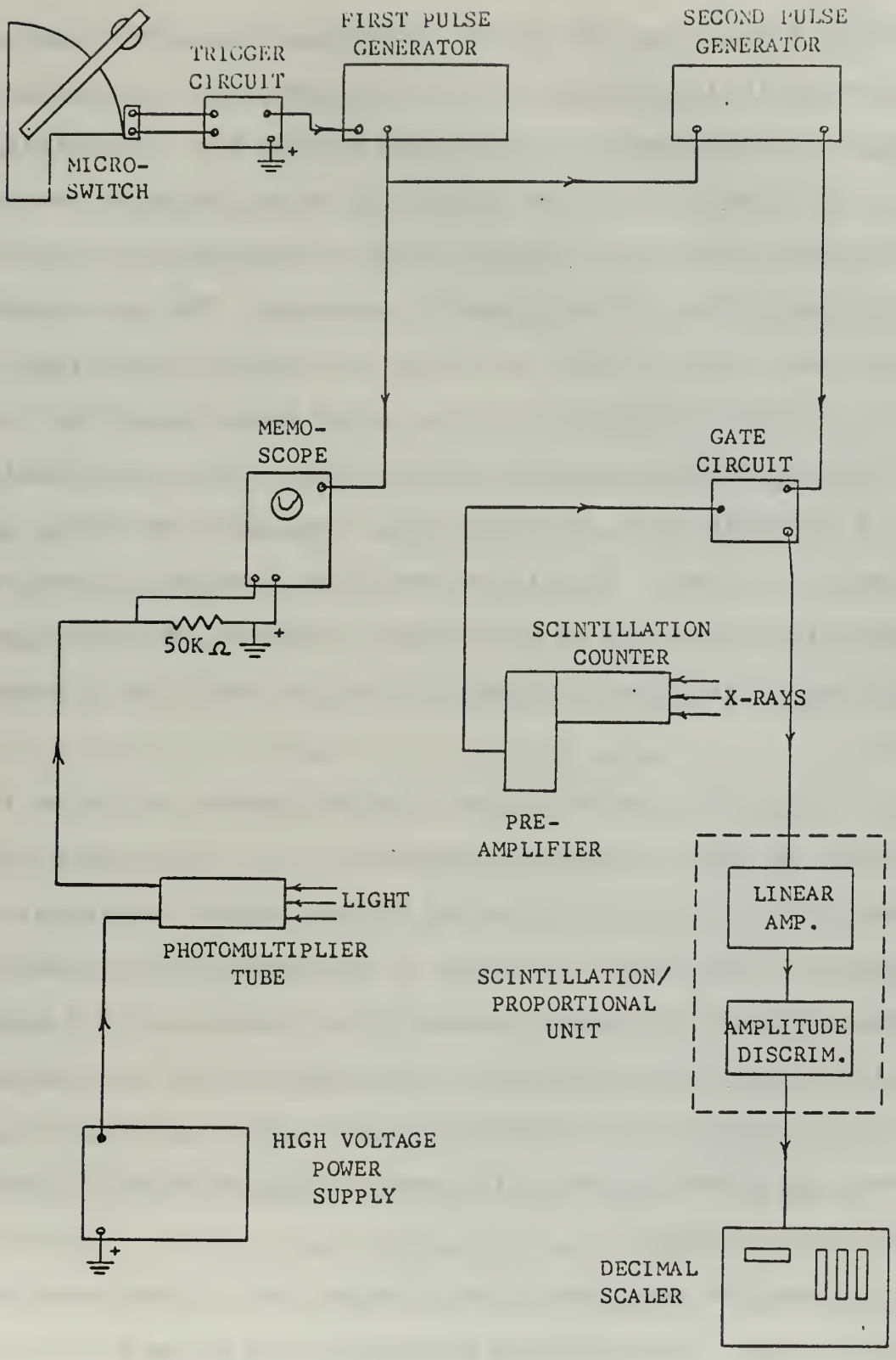

FIGURE 9. SCHEMATIC OF INSTRUMENTATION

range from 15 to 100 counts per second depending upon photomultiplier voltage. For the short counting periods used in this investigation, background counts were negligible.

In order to provide sufficient pulse strength for the following electronic circuits, the scintillation counter has a pre-amplifier as an integral component. The pre-amplifier provides a gain of 30. As shown in Figure 9, the signal from the pre-amplifier was fed to a linear pulse amplifier located in the Scintillation/Proportional Unit. The linear amplifier is a variable gain, two-tube pulse amplifier providing gains from 200 to 600. The linear amplifier provides linearity of amplification up to 80 volts with a minimum of distortion. The amplified signal is then fed to the amplitude discriminator.

Since all counters have a certain amount of noise inherent in their design and operation, it is desirable to have some method for discriminating between noise and signal pulses. This is the function of the amplitude discriminator. When adjusted for maximum sensitivity, pulses of 7-8 volts will fire the discriminator. The heart of the discriminator circuit consists of a Schmitt trigger which produces a constant amplitude output pulse when the input pulse is above the preset value.

From the amplitude discriminator one of two paths can be followed. Depending on the count rate being received the pulses can go directly to the counting device or through a scaler. The scaler in the Scintillation/Proportional Unit

consists of three binaries all of which perform the same function, that of dividing the number of pulses in the incoming signal by two, passing only the alternate ones. The first two binaries have resolution times of one microsecond and the third binary has a resolution time of five microseconds. In this investigation it was found unnecessary to use the binary stages.

The counter used to record the counts from the Scintillation/Proportional Unit was a decimal scaler shown in Figure 12. This counter registers pulses electronically to 999 and electromechanically to 9,999,999. It has a maximum average counting rate of 100,000 counts per second and will respond to pulses of one microsecond rise time or less with a pulse amplitude between 0.25 and 150 volts.

In order to count pulses from the scintillation during the desired time interval a triggering and timing circuit had to be devised. The triggering circuit is shown in Figure 10 and the timing arrangement is shown in Figure 9. The trigger consists of a normally open microswitch which is closed by the pendulum just before the two test surfaces came together squeezing the oil film. The pulse from the triggering arrangement provides the trigger to drive the first of two pulse generators. These pulse generators can be set for pulse durations from 0.1 microseconds to 1.0 seconds. The output from the first pulse generator consists of a delayed sync pulse which comes at the end of the main pulse. The delayed sync pulse serves two functions. First, it triggers the

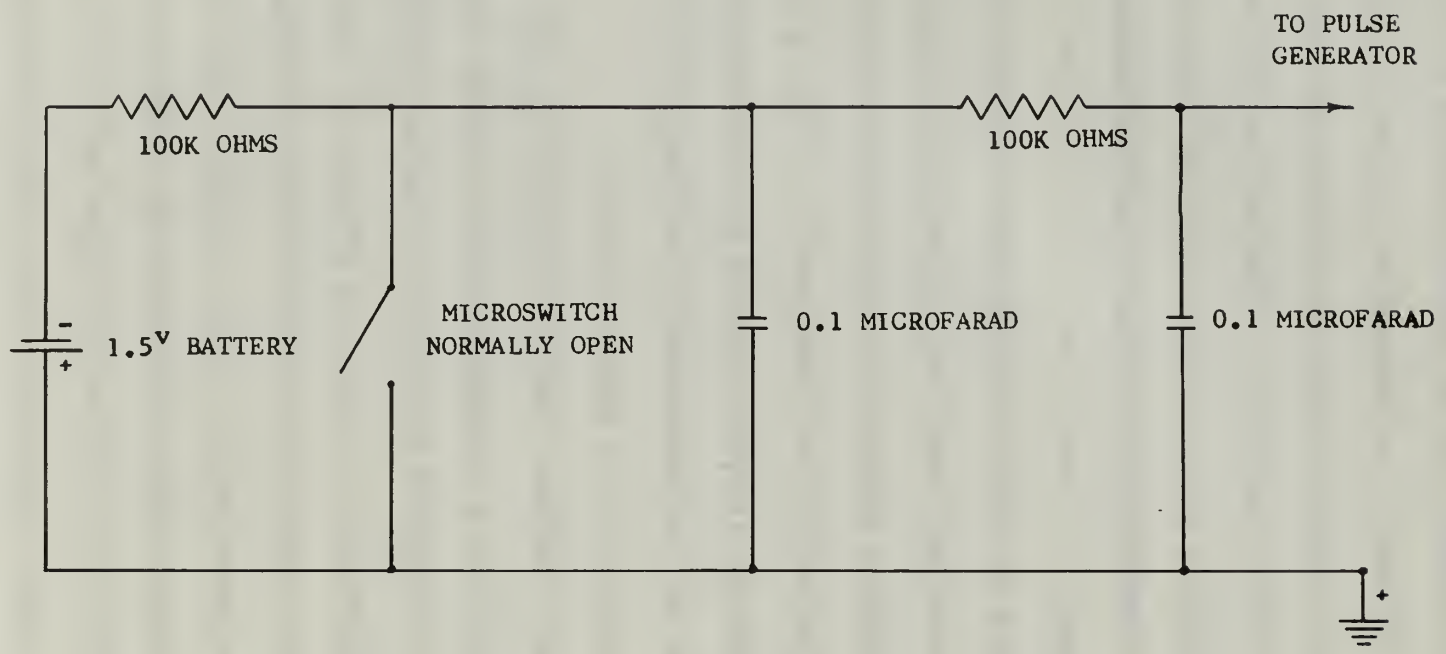

FIGURE 10. SCHEMATIC OF SINGLE-PULSE GENERATOR

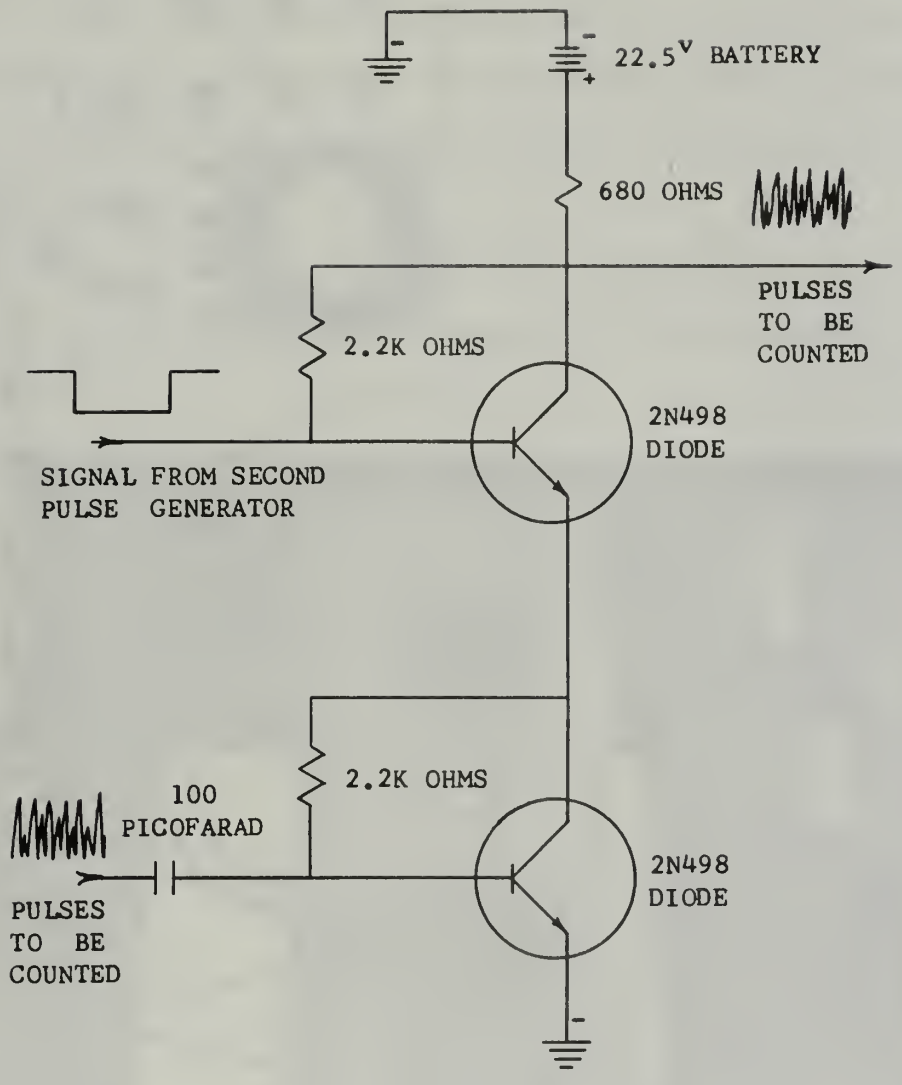

FIGURE 11. SCHEMATIC OF GATE CIRCUIT

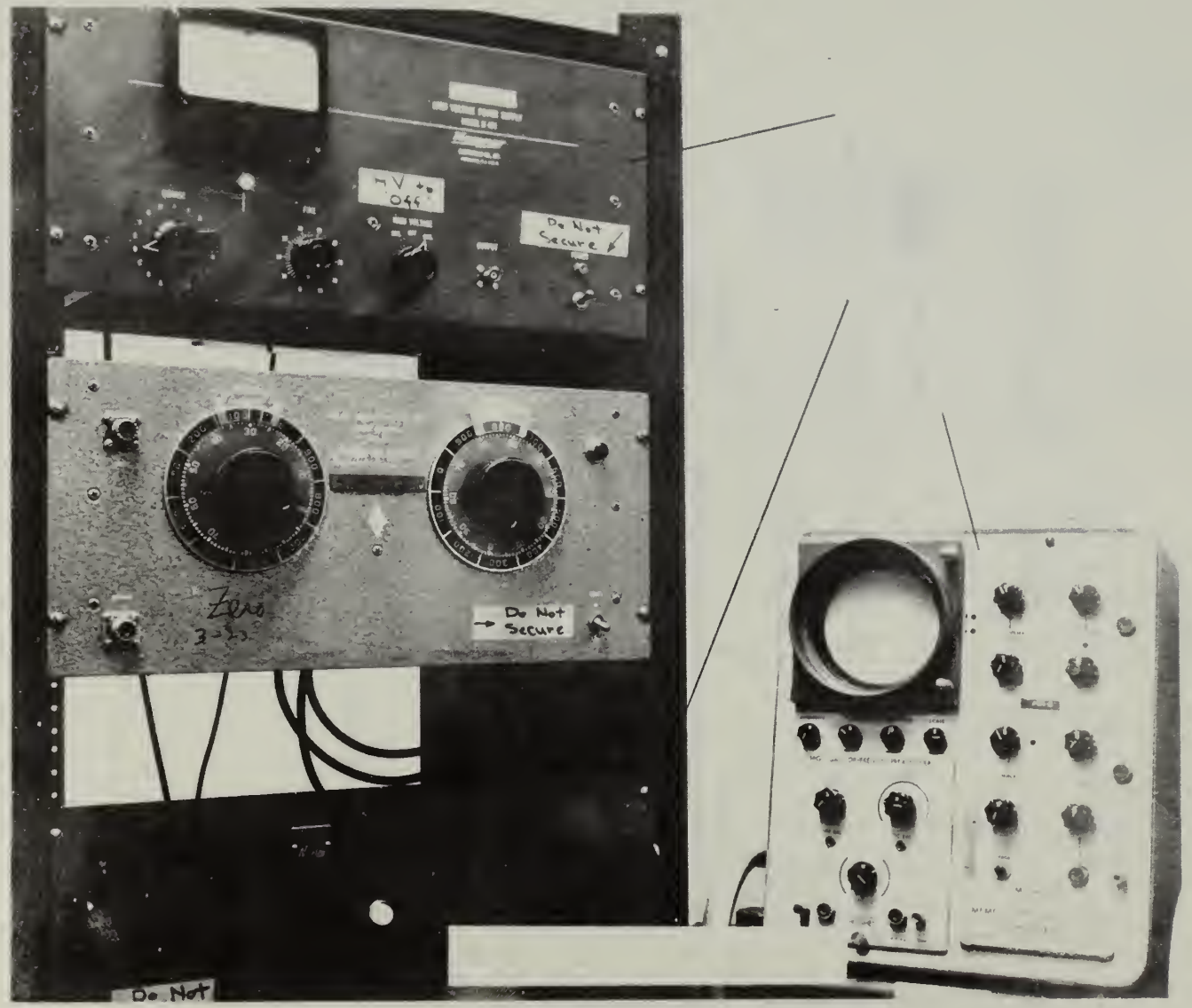
-V
Do Not Secure
Do Not Secure
Do Not

memoscope so that the signal from the light system will be recorded. Secondly, it triggers the second pulse generator. The function of this pulse generator is to provide a positive pulse of an adjustable duration which opens a gate circuit allowing pulses from the Scintillation counter through to the Scintillation/Proportional Unit. The gate circuit used is shown in Figure 11.

Thus by setting a specified delay time on the first pulse generator, a desired portion of the oil film variation may be observed. The desired delay time was such that the memoscope and gate circuit were triggered during the period of minimum film thickness. Then, by setting an appropriate counting time on the second pulse generator, counts will be passed through the gate circuit only during the duration of minimum film thickness.

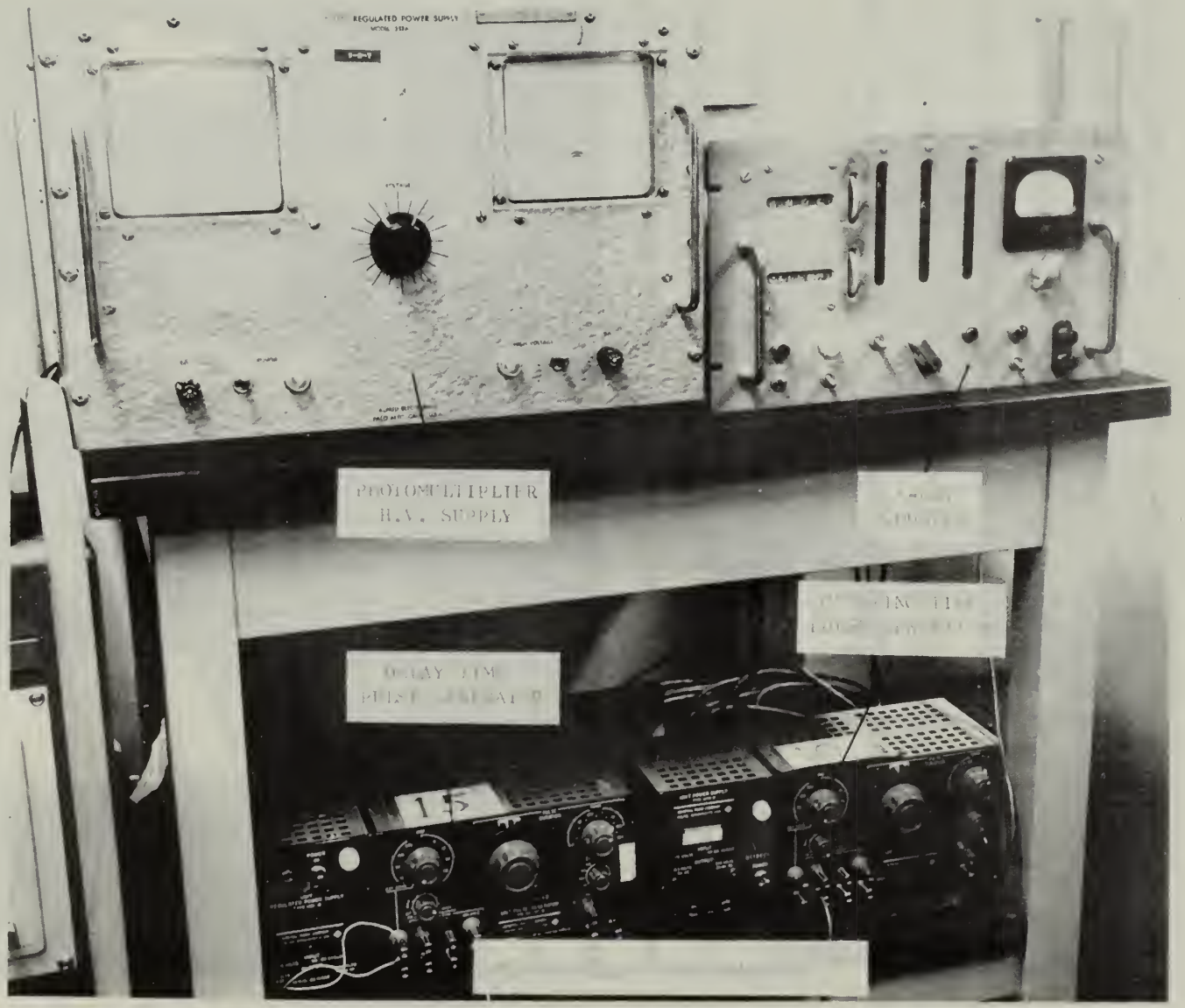
REGULATED POWER SUPPLY
PHOTOMULTIPLIER
H.V. SUPPLY

5. Calibration

In order to relate the raw data collected during testing to the desired information, that is oil film thickness vs. viscosity, speed or load, the test apparatus had to be calibrated. The basic objective of the calibration was to determine the variation in signal from the light and x-ray source with changes in oil film thickness between the two cylindrical disks.

For the light system, calibration was a relatively straightforward process. The signal output from the photomultiplier is directly proportional to the light signal incident upon it. Since the beam width of the light signal incident upon the photomultiplier tube is constant, the only way to vary the signal is to vary the gap setting thereby changing the strength of the light signal. This indicates that the output from the photomultiplier tube is directly proportional to the gap setting between the two disks. By observing the output of the photomultiplier tube on the memoscope shown in Figure 13, values of voltage vs gap setting may be obtained and calibration curves then plotted.

The calibration should then consist of setting known gap separations between the two disks with an oil film present and measuring the light and x-ray signal outputs. Since the initial objective of this thesis was to measure film thicknesses on the order of magnitude of microinches, a visual method of setting and determining gap separation was deemed to be too inaccurate. The calibration arrangement finally

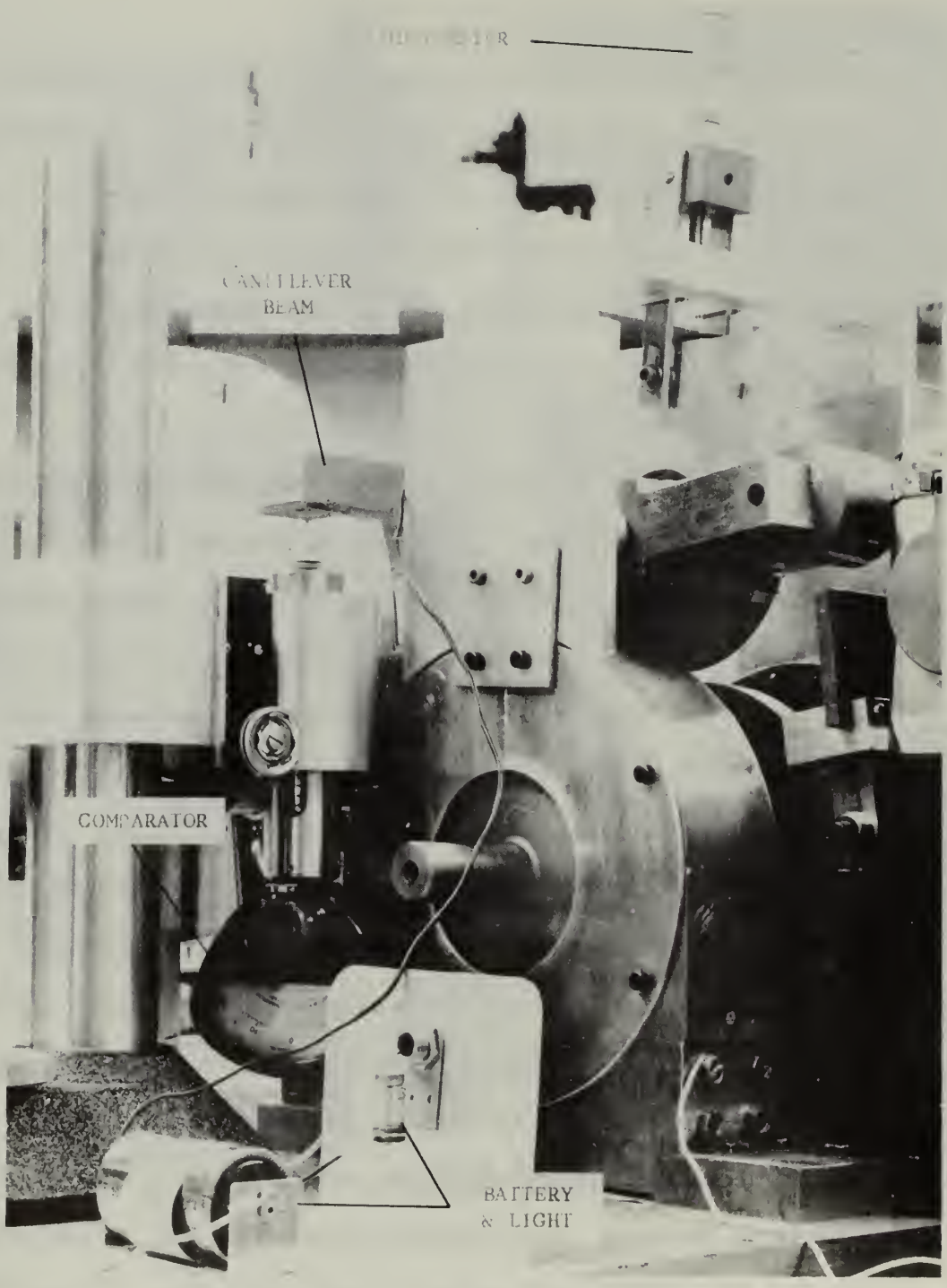

FIGURE 14. CALIBRATION ARRANGEMENT

settled upon is shown in Figure 14.

To adjust the gap separation between the disks a micrometer was used. The micrometer stem rests on a steel ball which rests in the cross arm and is a rigid member of the lower disk assembly. The steel ball was used so that the micrometer would make a point contact with the lower assembly and avoid "walking" of the micrometer and resulting relative motion between disks as the micrometer stem was turned. The pendulum and upper disk were attached to the micrometer by a cradle assembly so that as the micrometer was adjusted, the pendulum could be raised or lowered.

The method used to establish a known gap and measure the change in this gap between the two disks was an electrical circuit, as shown in Figure 15, and a comparator. An electrical circuit can be established between the two disks at the point of contact of the disks. This was accomplished by placing masking tape between the bearing hangers of the lower disk and the base plate so that the lower disk was completely insulated from the rest of the test apparatus.

The next step in the calibration procedure is to determine the actual gap separation between the two disks. To do this we must now consider dielectric strength of insulators which is defined as the maximum permissible electric intensity or electric potential gradient the insulator may sustain. Attwood [12] discusses this problem of dielectric strength. The dielectric strength of any insulator is measured by placing the insulator between two flat, parallel plate

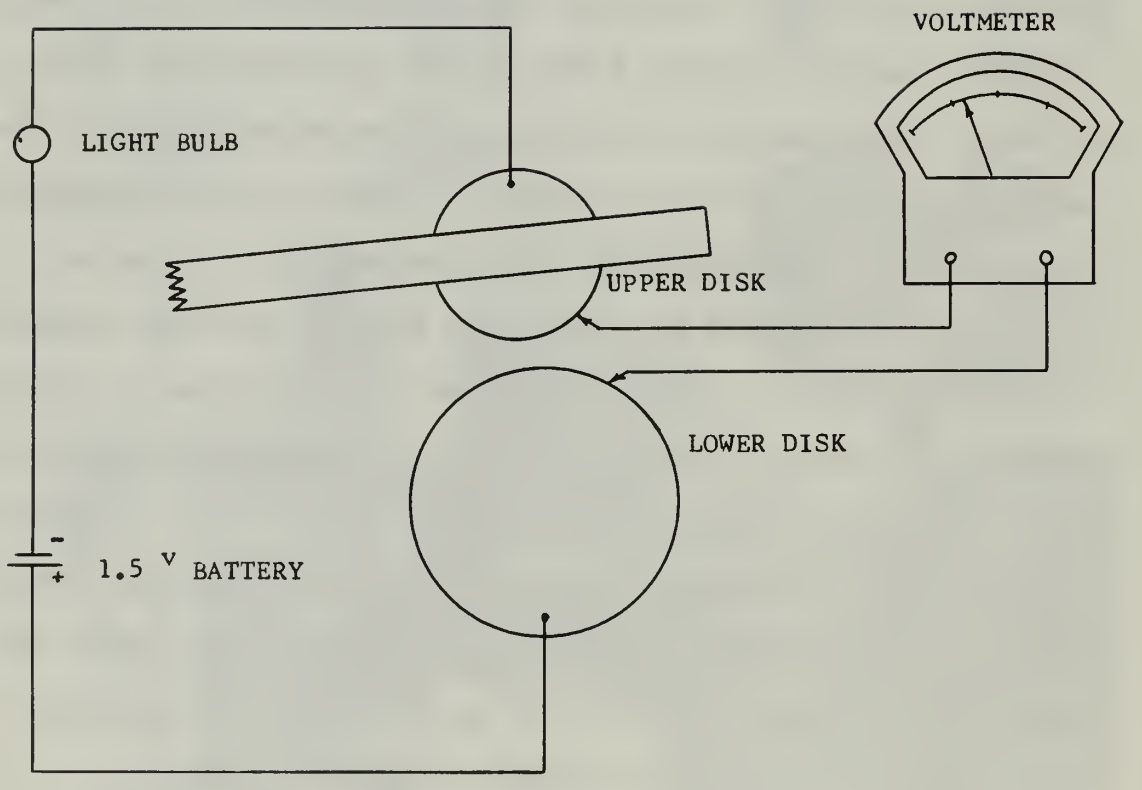

FIGURE 15. ELECTRICAL CALIBRATION CIRCUIT

electrodes. A voltage is then applied between the electrodes so that a uniform potential gradient is obtained across the insulator. By knowing accurately the separation between the electrodes, i.e. the insulator thickness, and the potential at which the insulator breaks down, the dielectric strength of the insulator is calculated. The dielectric strength of various insulators are generally well known values. For air at atmospheric pressure, the dielectric strength is 30×10^6 volts/meter. With this information the problem of gap settings may now be solved.

By applying a known voltage across the two cylindrical disks and adjusting the upper disk to the point where the electrical circuit is just broken by the air gap between the disks, a disk separation can be calculated:

$$\text{Disk Separation} = \frac{\text{Voltage across disks}}{\text{Dielectric strength}}$$

It must be remembered that the value of dielectric strength is valid only for cases where the electric field between the two surfaces is uniform. A uniform field can only be approached between circular disks if the separation between the disks is relatively small compared to the radius of curvature of the two disks. As an example, in the calibration tests, a voltage of 1.09 volts was measured between the two disks at the point where the circuit was broken. This indicates a gap separation of 14.3 microinches which certainly is small compared to a radius of curvature of 2.0 inches for the smaller disk or 3.0 inches for the larger disk. Thus,

the assumption that there is a very nearly uniform electric field at the closest point between the two disks should be valid. This in turn indicates the value of dielectric strength should be fairly accurate in order to calculate the disk separation.

Knowing the separation between the two disks accurately the next problem is how to measure the change in separation accurately. To do this a comparator, shown in Figure 14, was used. Full scale deflection is .0004 inches and each division is five microinches. The comparator rides up underneath a cantilever arm rigidly bolted to the pendulum. As the pendulum is raised or lowered, readings can be obtained to the nearest two microinches of any change from the initial disk separation.

To calibrate the test apparatus for a given oil, the disk surfaces were first cleaned with acetone. Then the disk separation is adjusted to the point where the electrical circuit between the disks is just broken. The potential between disks was measured and recorded and the oil was then placed between the disks using a hypodermic needle as shown in Figure 16. Readings were then obtained from the memoscope of millivolts versus gap separation between the disks. The results of this calibration is shown in Figure 17.

In calibrating the x-ray system, the same general technique is followed. The number of pulses per unit time coming from the pre-amplifier of the scintillation counter are directly proportional to the number of x-rays striking the

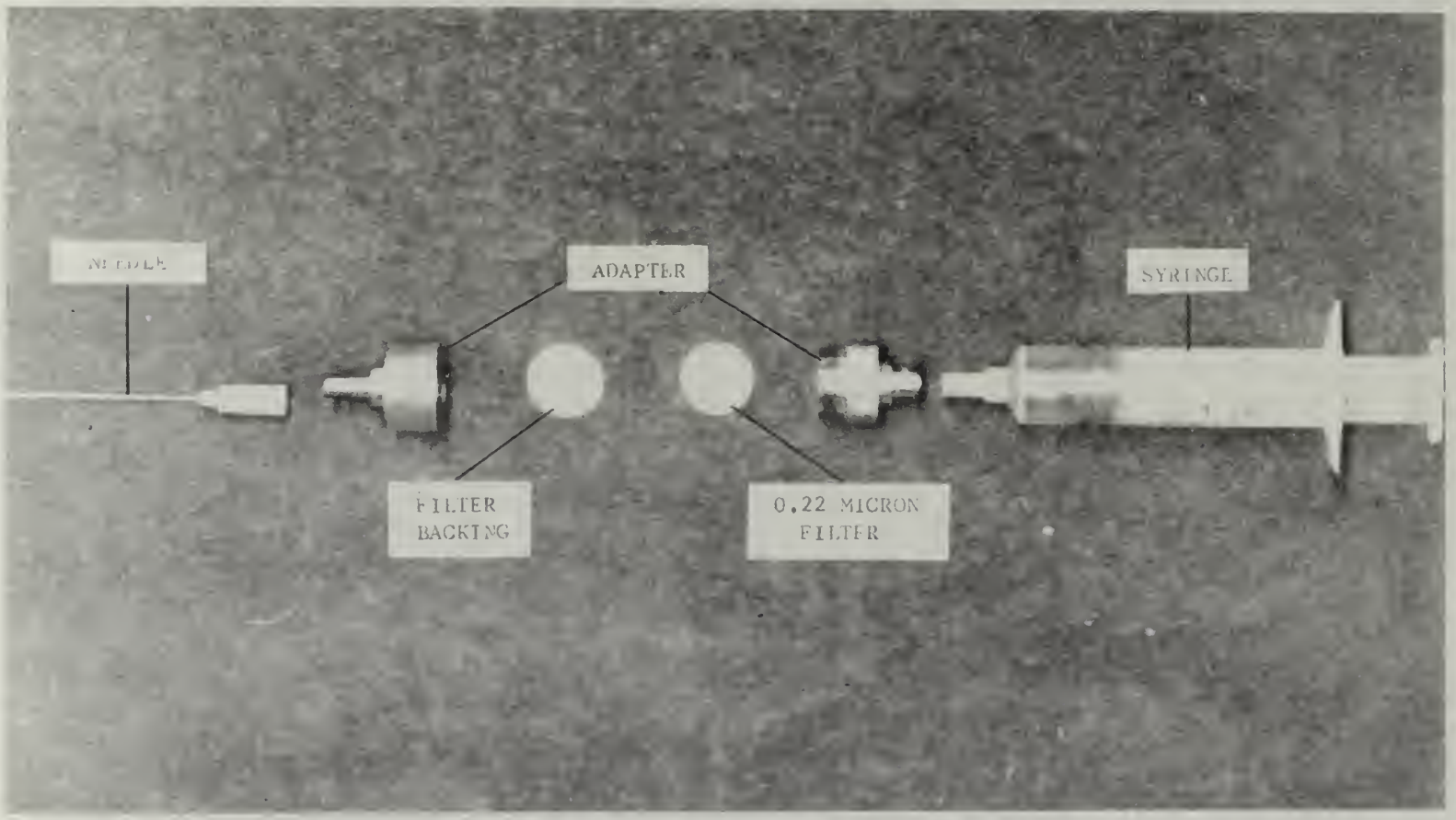

FIGURE 16. HYPODERMIC SYRINGE FOR FILTERING OIL

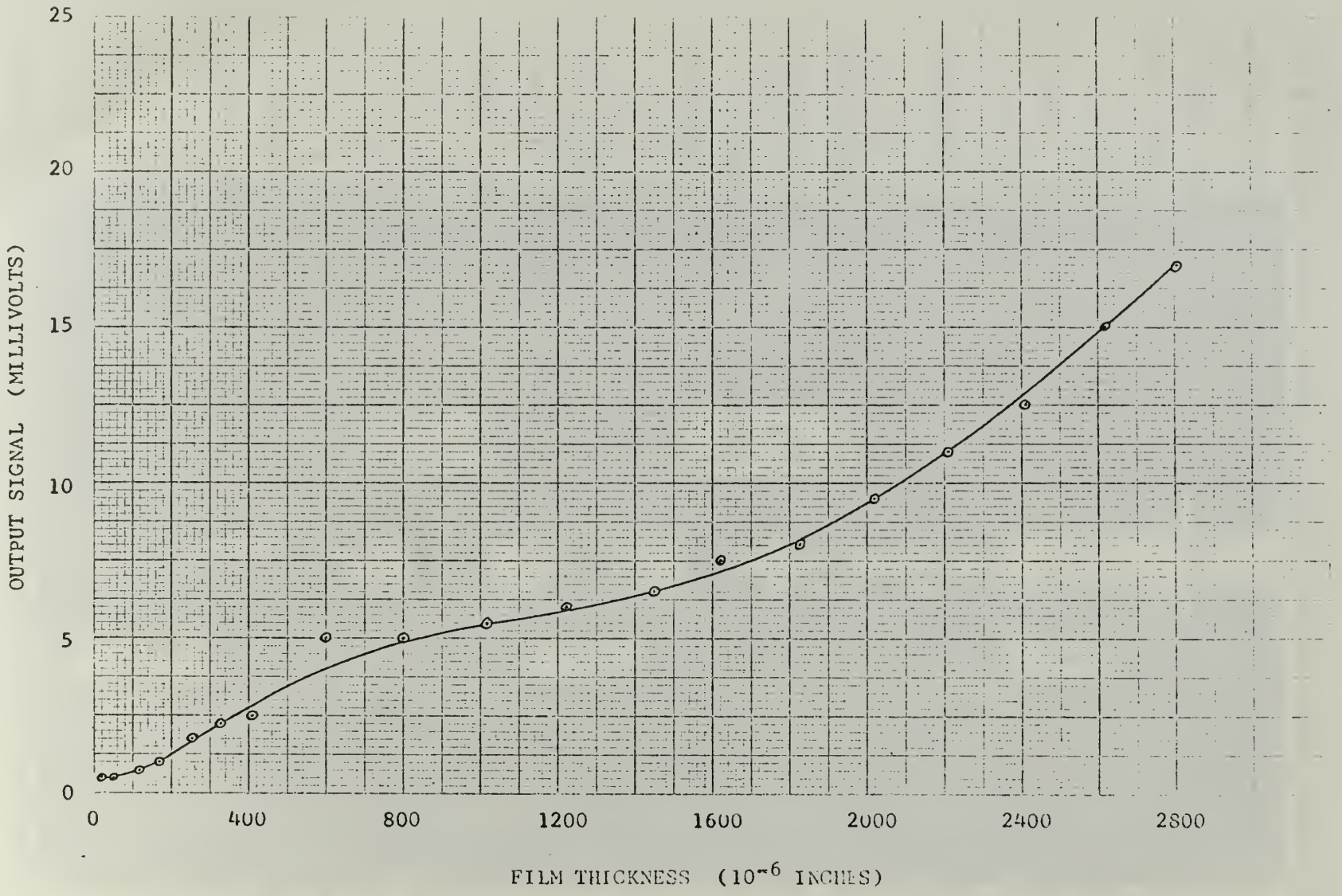

FIGURE 17. CALIBRATION CURVE FOR LIGHT SYSTEM

florescent crystal. In a similar manner to the light system, the number of x-rays striking the fluorescent crystal are proportional to the gap separation of the disks since the x-ray beam width is constant.

The apparatus used to measure and set the gap separations for the x-ray calibration is the same as was used for the light calibration. The apparatus used to measure the pulses per unit time for each gap setting was described in the proceding section. By setting the pulse generator for a set pulse length, the decimal scaler can be activated for a prescribed time interval. The number of counts obtained during this time interval will register on the decimal scaler. With this information, calibration curves as shown in Figure 18 of pulses per unit time versus gap separation may be obtained. As may be observed, the calibration curve below 400 microinches cannot be accurately interpreted. Since the initial aim of this study was to investigate the region down to 20 microinches film thickness, a second calibration curve was made. This curve, shown in Figure 19 was obtained by bypassing the discriminator and going directly from the linear amplifier to the counter. The gain of the linear amplifier had to be reduced to its lower limit so that the high count rate would not overload the counter.

Since the generation of x-rays is a random process and therefore subject to some fluctuation of x-ray intensity, calibration data was obtained by taking 15 readings at each setting of disk separation.

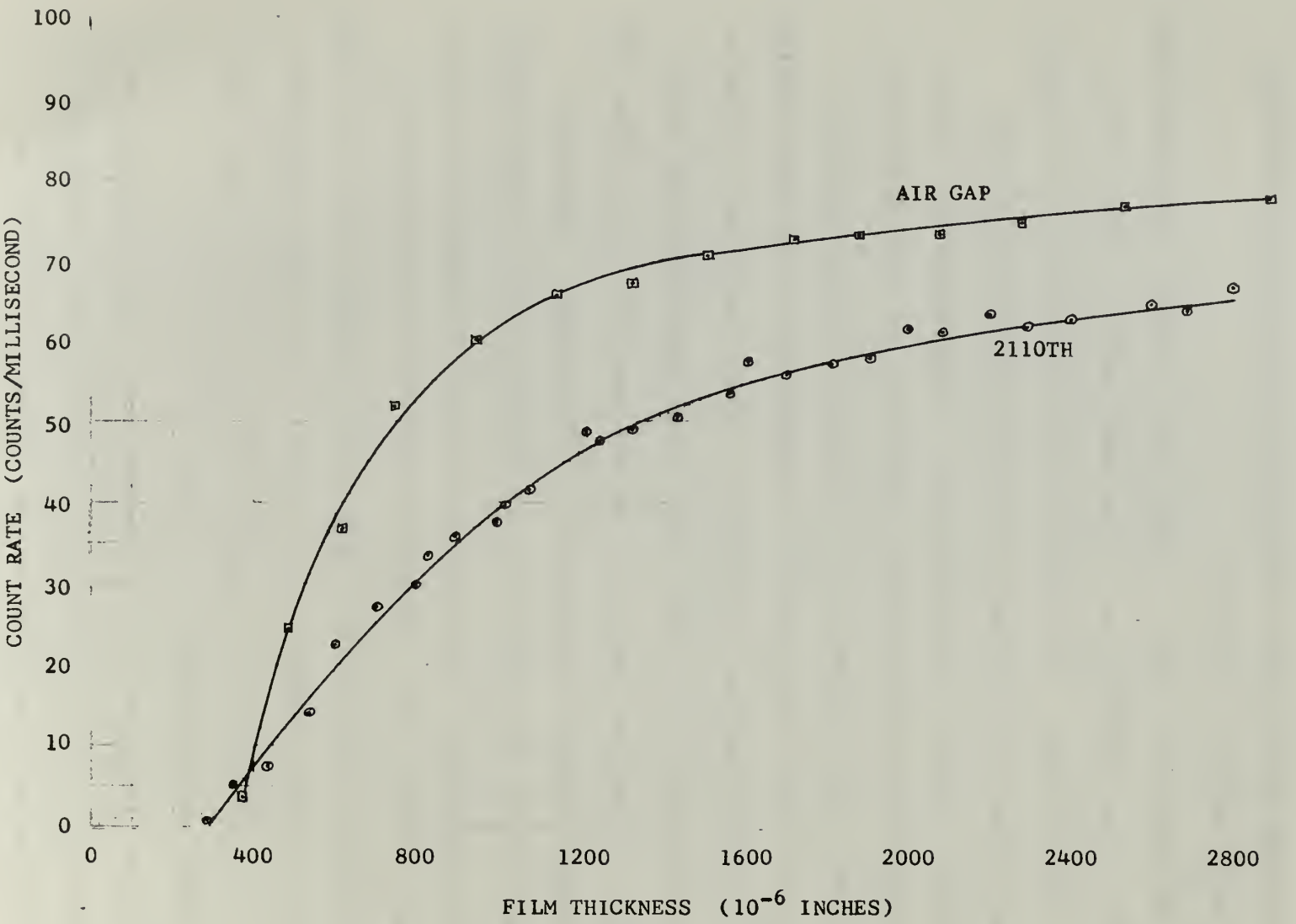

FIGURE 18. CALIBRATION CURVE FOR X-RAY SYSTEM USING DISCRIMINATOR

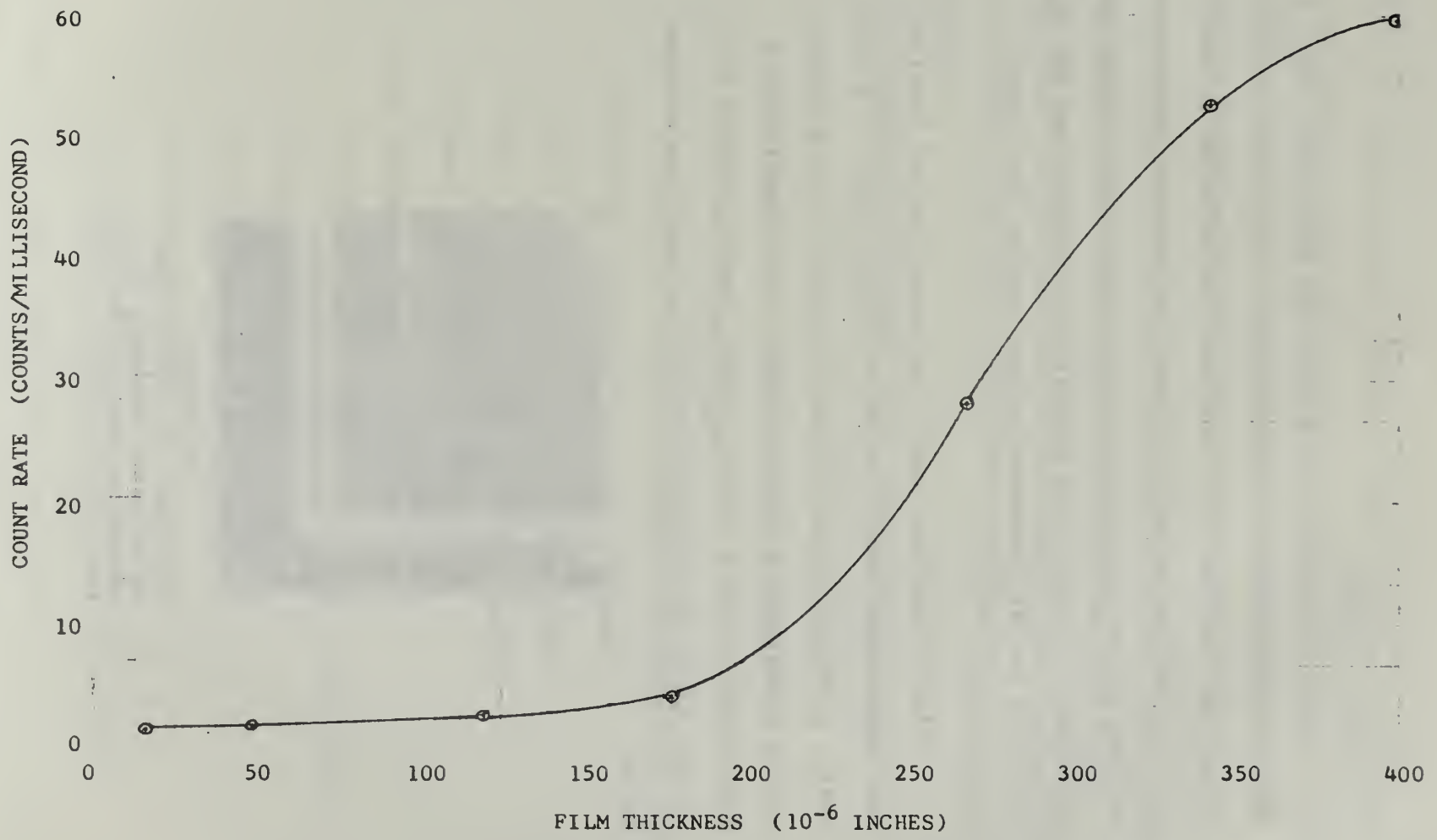

FIGURE 19. CALIBRATION CURVE FOR X-RAY SYSTEM WITHOUT DISCRIMINATOR

6. Test Procedure

In order to obtain consistent and meaningful data, a test procedure had to be established. The first step required was to turn on all equipment and allow it to warm up for a minimum of half an hour. In practice, this warm up time turned out to be more nearly one hour. During this time high voltage to the scintillation counter was set at 800 volts and all instruments were checked for proper connections.

Prior to any test runs being made, the D-C level of the light signal had to be set to a zero point. In early tests, a phenomena was noticed which had to be accounted for in establishing the zero point. In establishing a zero point and then running a test, there appeared to be an over shoot of the signal below the zero line as shown below.

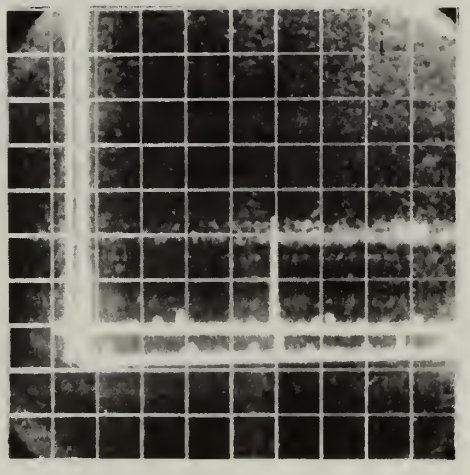

FIGURE 20
Overshoot of light signal below zero reference line. Both test surfaces dry and lower disk slowly rotating.

This is apparently a characteristic of the circuitry in the photomultiplier tube such that when the light signal is suddenly cut off, the signal from the photomultiplier tube drives negative by about four millivolts. The zero line on the memoscope was established by placing the test surfaces together so that no light signal was detected and then placing the D-C level four millivolts above the desired zero line. The zero line was periodically checked to insure its correctness.

In conducting the tests, the following procedure was used:

(a) Clean test surfaces with acetone

(b) Set pendulum height

(c) Set drive motor at constant preselected value

(d) Apply lubricant to test surface

(e) Set delay time and counting time

(f) Set decimal scalar to zero counts

(g) Arm sweep on memoscope

(h) Darken room

(i) Bring photomultiplier tube up to 900 volts

(j) Turn on light source

(k) Turn on x-ray source

(l) Release pendulum

(m) Photograph trace on memoscope and record counts

In conducting test runs for a given set of conditions, an initial run was made to determine the time at which minimum film thickness occurred and the duration time of

minimum film thickness. The delay and counting time periods were then adjusted on the pulse generators for subsequent tests. These times were set so that the memoscope would trigger at the start of the minimum film thickness period and the counter circuit would operate only during this period of minimum film thickness. The results of these tests are described in the following section.

7. Experimental Results

As has been previously stated, the purpose of this investigation was to examine the behavior of thin oil films. Relating theoretical considerations with previous experimental work with 2110TH lubricants, it became apparent that the criteria for obtaining thin oil films would be slow rotative speeds and high loads. For this reason, tests were conducted at rotative speeds of 50, 100, 150, and 200 RPM using drop angles of 5.5 and 10.25 degrees for the pendulum. The results are shown by the photographs taken on the memoscope along with the counts recorded by the decimal scaler.

In observing the results of the tests, several points should be recognized:

(a) The time scale is arbitrarily selected to obtain an optimum trace. The zero point or start of the trace sweep was also arbitrarily selected to obtain an optimum trace. The zero point remained fixed for all tests.

(b) The circuitry was set up so that the signal from the photomultiplier tube was positive. Therefore, as the pendulum was dropped, cutting off the light through the oil, the signal dropped from a positive value toward the zero reference line.

(c) The zero reference line for the ordinate was positioned and the scale chosen to obtain an optimum presentation. In order to relate voltage readings, in millivolts, to oil film thickness,

the calibration curve shown in Figure 17 must be used. Since the calibration curve is non-linear, annotated conversion factors are not used.

(d) All data obtained from the x-ray system was with the discriminator in the system. Therefore, Figure 18 must be used to relate x-ray data to oil film thickness.

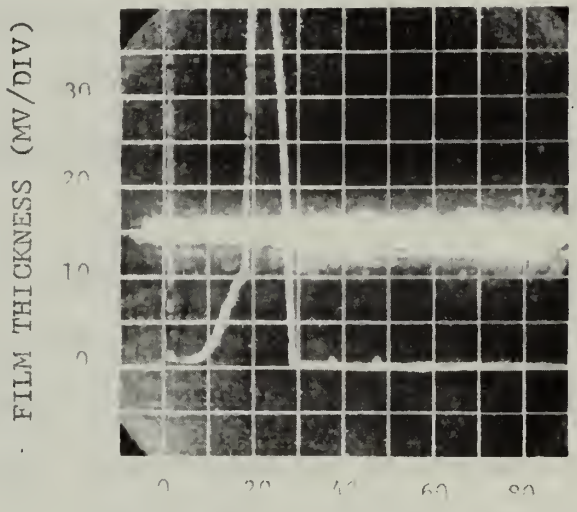

FIGURE 21.

In the tests shown in Figure 21 oil was placed on the lower test surface with it rotating at 50 RPM. The upper disk was dry and the pendulum height was set at 5.5 degrees. The trace represents the velocity at which the upper test surface strikes the lower test surface. Note the high speed, represented by the first nearly vertical line at the left of the picture, at which the test surfaces hit.

The first flat part of the trace is slightly less than one millivolt above the reference indicating a film thickness of about 150 microinches. The next vertical line to the right shows rebound of the pendulum and upper disk. Note the slower separation velocity as the test surfaces recover from elastic deformation. The rate of separation then increases as the rebound continues. The right hand vertical line shows the upper disk again falling and striking the lower disk. This time there is no rebound and the two disks remain in contact. The slight decrease in trace down to the reference line shows the oil being squeezed out the sides of the two disks. Counts from the x-ray system were 80 counts per millisecond. This reading was too high to obtain a count from the calibration curve.

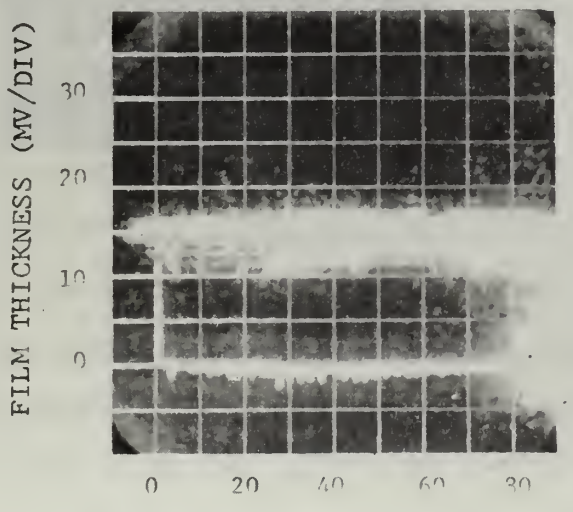

FIGURE 22.

The next series of tests as shown in Figure 22, were run at 50 RPM with the pendulum raised to 10.25 degrees. Note how the trace comes down nearly vertically to the reference line without rebounding. From this trace it appears that the oil film is very thin - making it impossible to interpret from the light system. 65 counts per millisecond were obtained from the x-ray system indicating a film thickness of about 2800 microinches. The light area in the middle of the picture is merely where the memoscope has been used too many times leaving a permanant trace.

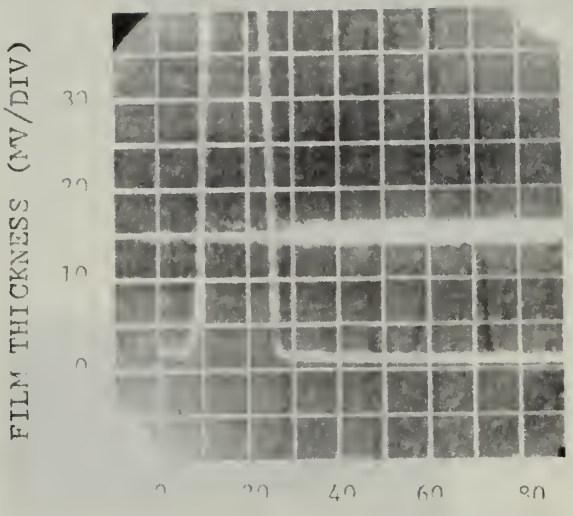

FIGURE 23.

The next series of tests, represented by the trace shown in Figure 23, were conducted at 100 RPM and a pendulum drop

angle of 5.5 degrees. This trace begins during the period when the oil film is being squeezed and shows a reading of about 2.0 millivolts corresponding to a film thickness of 300 microinches. The x-ray system gave a count of 100 counts per millisecond which could not be interpreted on the calibration curve. Again, notice the rebound obtained with this low angle drop.

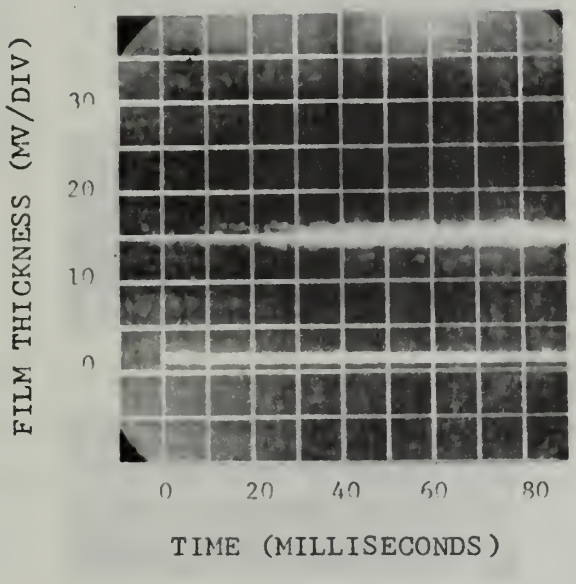

FIGURE 24.

The trace shown in Figure 24, represents the series of tests run at 100 RPM and a pendulum drop angle of 10.25 degrees. This trace starts right after the two test surfaces have come into contact, squeezing the oil film. The light system again indicates about 2.0 millivolts or a film thickness of 300 microinches. For this particular run,

the x-ray system indicated 13 counts per millisecond or a film thickness of 400 microinches. This was the type of corresponding data which was expected from all test runs. As can be seen from the preceding and following traces, this was not always the case. Some variation was expected in the counts from the x-ray system due to randomness of x-ray emission, but not the wide range of counts actually obtained.

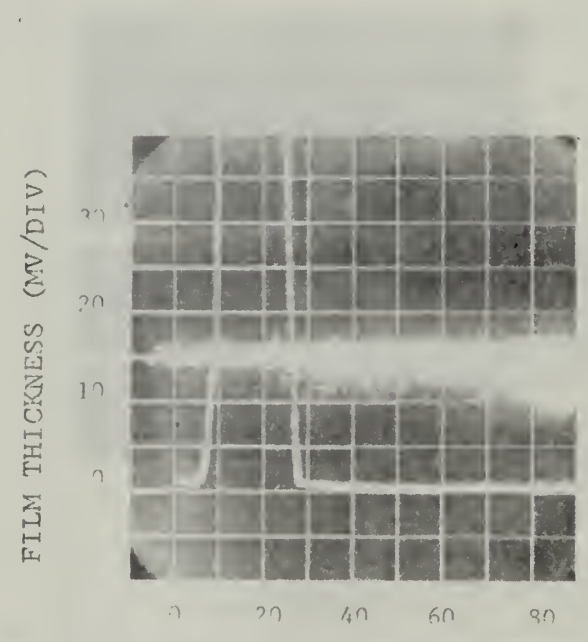

FIGURE 25.

The trace in Figure 25 shows the next series of tests run at 150 RPM and pendulum drop angles of 5.5 degrees. This trace indicates a film thickness of 1.0 millivolts or about 170 microinches. The counts from the x-ray system were 8

counts per millisecond indicating a film thickness of 400 microinches. Again note the rebound from the low angle drop.

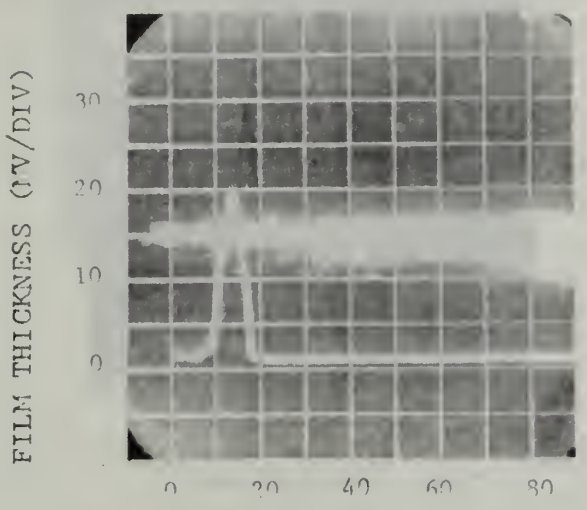

FIGURE 26.

The next series of tests, shown by the trace in Figure 26, were run at 150 RPM and pendulum drop angles of 10.25 degrees. This trace shows a reading of about 2.0 millivolts from the light system corresponding to a film thickness of 300 microinches. Note the slight rebound obtained with slightly higher speeds and high drop angles. 100 counts per millisecond were obtained from the x-ray system and could not be interpreted from the calibration data.

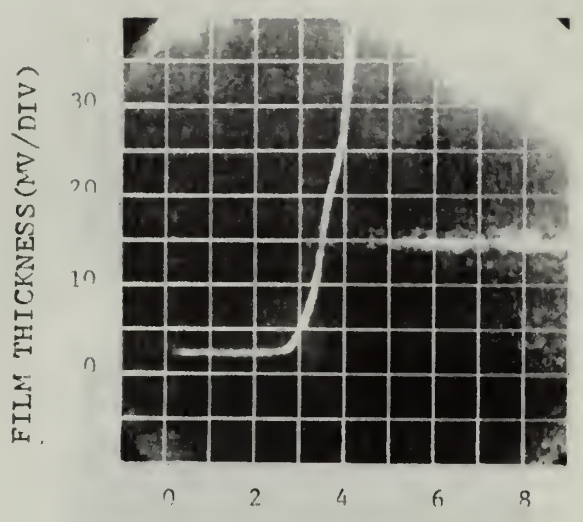

FIGURE 27.

The trace shown in Figure 27 represents the next series of tests run at 200 RPM and pendulum drop angles of 5.5 degrees. The time scale was expanded on this series to obtain better definition of minimum film duration. The light system here indicates a film thickness of 2.5 millivolts or 370 microinches. The x-ray system, however, gave 137 counts per millisecond which could not be interpreted from the calibration data.

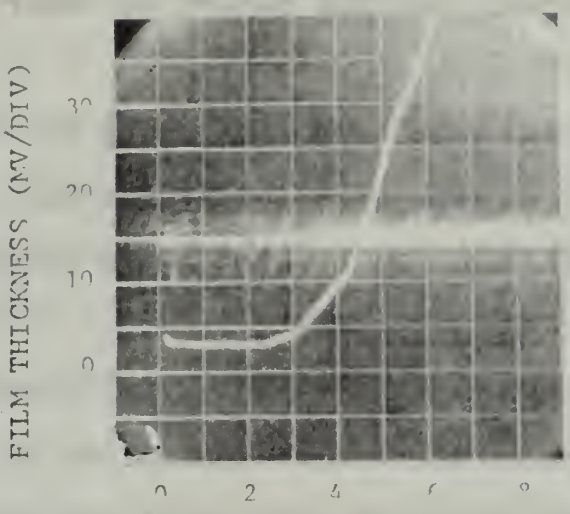

FIGURE 28.

The last series of tests represented by the trace shown in Figure 28, were run at 200 RPM with pendulum drop angles of 10.25 degrees. An expanded time scale was again used on this series of traces. The light system shows a reading of 3.0 millivolts corresponding to a film thickness of 440 microinches. The x-ray system, however, counted 83 counts per millisecond which was too high to be interpreted by the calibration data. The difference in the rebound of the last two series of tests should be noted. The slower rebound obtained with higher pendulum drop angles appears to be caused by the greater deformation of the two test surfaces.

This deformation causes the thin film to be held slightly longer while the deformed surfaces return to their original shape.

A total of 109 test runs were made using the 2110th lubricant. Of these, 61 runs were successful for obtaining data from the x-ray system. Below is shown a tabulation of the results obtained from the x-ray system.

The values of speed given are the rotative speed of the lower disk at the time of the test. The values of drop angle show the angle through which the upper disk was dropped to squeeze the oil film. The tabulation of counts shows the spread of results between the high and low values. The number of runs indicate the number of tests under the load and speed conditions for which useful x-ray information was obtained.

Speed (RPM)	Drop Angle (Degrees)	Counts/Millisecond		No. Runs
		Low	High	
50	5.5	13	106	7
	10.25	33	97	7
100	5.5	6	106	17
	10.25	10	97	7
150	5.5	12	70	8
	10.25	41	103	5
200	5.5	30	186	6
	10.25	4	117	4

8. Discussion of Results

In any work of an experimental nature, the results must fall within some reasonable limit and be repeatable. This was not the case for the x-ray technique used. Observation of the table of x-ray counts per millisecond compared to load and speed conditions indicate that there is an unacceptable spread in the data. This would seem to indicate the infeasibility of using an x-ray technique to measure lubricant film thicknesses under short duration loads. At this point, it should be noted that this investigation was spurred by the work of Sibley and Orcutt with x-rays. However, their work was done under steady load conditions with counting periods of 15 seconds.

It seems that any attempt to analyze the results of this work must consider: (a) ability of the test equipment to operate satisfactorily under the required conditions; (b) instability or large variations in the x-ray signal; or (c) occurrence of some unexpected phenomena.

Considering the test equipment first, one must start with the scintillation counter. As previously mentioned, the dead time of the scintillation counter used was about 0.2 microseconds which ensures linear counting up to very high intensities. The primary limitation of scintillation counters is generally the decay time of the phosphor. In this case the fluoresence decay time is about 0.1 microseconds which accounts for the extremely high count rate capability.

The next suspect would be the pulse generators and gate circuit used to control the signal from the scintillation counter to the Scintillation/Proportional Unit. In anticipation of the response times required for this technique, a solid state gate circuit was used. The response time for a circuit of this nature is on the order of 50-100 microseconds which is reasonably small when compared to the counting times of one millisecond or greater. After obtaining the random results of the first few tests, the pulses from the pulse generators were checked. The desired pulse durations appeared very accurate. The rise and fall times for the pulses are normally less than 20 nanoseconds - typically 12 nanoseconds. This seems to eliminate the possibility that the gate circuit may have operated for a longer period than desired.

This brings one to the Scintillation/Proportional Unit. Literature on the detailed specifications of this unit are very limited. The general design function of this unit, however, is to permit operation of the high speed scintillation and proportional counters with the low frequency electronic equipment normally used with Geiger counters. This is done by the use of three binaries which scales down the count. However, these binaries were not used in this work. The only parts of this unit which were used were the linear amplifier and discriminator. Although there are no figures on which to base this, it is felt that these two components were not a source of trouble.

The last basic item of equipment is the decimal scaler. As mentioned in the section on instrumentation the decimal scaler counts electronically to 999. The electronic counters have a capacity for counting periodic pulses up to 200,000 counts per second. For a random pulse rate, however, this capacity is reduced. Random pulse rates of 100,000 will approach the counting capacity of this scaler. This, however, is the maximum counting rate reached in this work and should not have any effect on the accuracy of these results. In review, there does not appear to be any one piece of equipment which was taxed beyond the limits of its capacity. It is felt, therefore, that electronic equipment did not contribute appreciably to error in the results.

The next area to be considered is the stability of the x-ray equipment. It should be noted at this point that some fluctuation of the x-ray signal was to be expected since the process of x-ray emission is a random process. In order to account for this, calibration curves were plotted by obtaining 15 readings at each setting of disk separation. Also, two calibration runs were made to observe the repeatability of x-ray counting.

An analysis of the reliability of x-ray spectrography is given by Liebbafsky, et al. [13] . Studying the reliability of the x-ray emission involves a comparison of standard deviation, S to standard counting error S_c .

Standard deviation is defined as

$$S = \sqrt{\Sigma_i (N_i - \bar{N})^2 / (n-1)}$$

where N_i is the counts obtained in each test, $\bar{N}$ is the mean number of counts, and n is the number of tests. The standard counting error is defined approximately by

$$S_c = \sqrt{\bar{N}}$$

This standard counting error is considered to be the irreducible minimum deviation for x-ray emission spectrography under ideal conditions. As shown above, this error is not only a minimum, but a predictable minimum. The useful criteria for evaluating results is that when the standard deviation significantly exceeds the counting error there are other errors superimposed upon the random fluctuations of x-ray emission. These errors could be drift in the emission, instability of the x-ray emission or large fluctuations in the x-ray emission pattern. A chart is shown below which compares the standard deviation and counting error, both in counts per millisecond, and disk separation in microinches under calibration conditions.

Disk Sep.	600	1025	1445	1835	2415	2815
S	3.68	5.2	6.25	4.8	4.58	2.3
S_c	4.72	6.3	7.4	7.55	7.9	8.2

Under calibration conditions, this seems to indicate a measurement of counts which is within the random x-ray emission tolerances.

The same information can be tabulated for the tests run under dynamic conditions. These results compare the standard deviation and counting error, both in counts per millisecond, for given rotative speed of the lower disk and drop angle of the upper disk.

SPEED RPM	DROP ANGLE DEGREES	S	S_c
50	5.5	36.0	7.87
	10.25	23.08	7.68
100	5.5	36.36	7.21
	10.25	34.14	8.00
150	5.5	21.81	6.40
	10.25	25.56	8.60
200	5.5	56.88	9.59
	10.25	48.46	8.46

This tabulation clearly shows that for all conditions of dynamic loading, the standard deviation significantly exceeds the standard counting error indicating some large deviation above the random x-ray emission. While the above results would instantly lead one to suspect the stability of the x-ray emission, the tabulated results from the calibration data indicate the x-ray emissions are stable with some slight randomness.

These results finally lead to the possibility of some unknown phenomena ocurring. Here one must theorize as to what possibilities might lead to widely varying data. The first possibility is that out of roundness of the lower

rotating disk may have affected readings by moving the thinly squeezed oil film up or down relative to the x-ray beam. This was recognized from the very start as a potential problem.

With this and the problem of alignment of a relatively massive test apparatus to a fixed x-ray beam in mind, an x-ray beam was used having a 10x12 millimeter focal spot. Alignment of the test apparatus was made such that the point of contact of the two test surfaces would be very nearly in the center of the x-ray beam. From the center of the beam to either the top or bottom of the beam is five millimeters or 0.197 inches. Out of roundness, measured at very slow rotating speeds, was determined to be 0.0002 inches. The intensity of the x-ray beam has a plateau in its center which drops off rather abruptly at the edges. From this it appears that out of roundness would have to be significantly greater than 0.0002 inches to obtain the effect of wide scatter in data.

Another possible source of trouble might lie in the fact that the light system does not give a sufficiently accurate presentation of just when minimum film thickness occurs. It must be remembered that the start of counting and duration of counting x-ray pulses was based on the presentation obtained from the light system. One of the basic assumptions was that the light system did give an accurate presentation of variation in oil film thickness. It still seems difficult to discount this assumption,

however, in considering all aspects, this possibility should not be ruled out.

In connection with this, it was noticed that during the tests, severe foaming and turbulence of the lubricant occurred at entrance to the thin film region. Smith [14] mentioned this phenomena in his study of rheological problems of lubricants. It is quite possible that this effect could have resulted in false signals from the light system. It could also have caused erratic readings from the x-ray system by affecting the path length of the lubricant in some complex manner.

In summary, the cause of the erratic data obtained is not clearly understood. It could be the result of one of the above-mentioned possibilities or a combination of several of them.

9. Conclusions and Recommendations

In theory, the technique of measuring thin oil films under dynamic loads by counting x-ray pulses for short time periods is good. As in so many engineering problems, theory and valid results are separated by a large number of variables. Investigation of this problem began with reasonable expectation of obtaining valid results. The final conclusion must be that the x-ray technique attempted in this investigation is unsatisfactory for the study of thin oil films under dynamic loads.

The application of x-rays to measurement of thin oil films should be recognized as a very powerful technique to solving many lubrication problems. Future investigation should, however, recognize the problems encountered in this investigation. There still appear to be several possible methods open to investigation of thin film lubrication using an x-ray technique. These both, more or less, seem to involve the use of continuous counting techniques.

One method would involve the use of a high speed tape recorder which could record the pulses obtained from the x-ray detector. This would have the important advantage of recording the rate of change of pulses through the oil film. In theory, this could be related to oil film thickness by calibration data. It does appear that this method would involve a complex technique of rather sophisticated equipment and computerization of data.

Another possible method involves the use of a

multi -channel scaler. This would provide a large number of counters, each counting over a very small time interval. This provides a semi-continuous method of x-ray counting during the period of minimum film thickness. Several problems must be considered in the method, however. Depending upon the capacity of the multi-channel scalar, the period of minimum film thickness still needs to be known quite accurately. Also, the intensity of x-rays must be sufficient so that counting can be done during short time intervals.

Provided equipment of the nature just described is available and no unforeseen problems arise, it is strongly recommended that future study in this field be continued.

BIBLIOGRAPHY

1. El-Sisi, S. I., and Shawki, G. S. A., Measurement of Oil-Film Thickness Between Disks by Electrical Conductivity, Jour. of Basic Eng., Vol. 82, No. 1, March 1960, p. 12.

2. Mac Conchie, I. O., and Cameron, A., The Measurement of Oil-Film Thickness in Gear Teeth, Jour. of Basic Eng., Vol. 82, No. 1, March 1960, p. 29.

3. Shiflette, W. M., Determination of Oil Film Thickness in Partial Sleeve Bearings by Electronic Means, USNPGS Thesis, 1949.

4. Klorig, W. N., An Investigation of Lubricant Film Thickness Under Condition of High Intensity-Short Duration Loading, USNPGS Thesis, 1965.

5. Hydinger, R. M., The Measurement of Oil Film Thickness Versus Time Under Impact Loading Conditions, USNPGS Thesis, 1966.

6. Sibley, L. B., and Orcutt, F. K., Elasto-Hydrodynamic Lubrication of Rolling-Contact Surfaces, ASLE Trans., Vol. 4, 1961, p. 234.

7. Grubin, A. N., Fundamentals of the Hydrodynamic Theory of Lubrication of Heavily Loaded Cylindrical Surfaces, Book No. 30, Central Scientific Research Institute for Technology and Mechanical Engineering, Moscow, 1949.

8. Dowson, D., and Higginson, G. R., New Roller Bearing Lubrication Formula, Engineering, 192 (4792), 158-159, August 4, 1961.

9. Sibley, L. B., Bell, J. C., Kannel, J. W., Allen, C. M., A Study of the influence of Lubricants on High Speed Rolling-Contact Bearing Performance, ASD Technical Report 61-643, August, 1961.

10. Ree, T., and Eyring, H., Theory of Non-Newtonian Flow. I. Solid Plastic System, Journal of Applied Physics, Vol. 26, No. 7, July 1955, p. 793.

11. Dowling, P. H., Hendee, C. F., Kohler, T. R., and Parrish, W., Counters for X-ray Analysis, Norelco Reporter, Vol. 4., No.2, March-April 1957, p. 23-33.

12. Attwood, S. S., Electric and Magnetic Fields, John Wiley & Sons, Inc., New York, 1958.

13. Liebhafsky, H. A., Pfeiffer, H. G., Winslow, E. H., and Zemay, P. D., X-ray Absorption and Emission in Analytical Chemistry, John Wiley and Sons, Inc., New York, 1960.

14. Smith, F. W., Lubricant Behavior in Concentrated Contact-Some Rheologhical Problems, ASLE Trans., Vol. 3, No. 1, p. 18.

15. ASME Pressure-Viscosity Report, Vols. I & II, New York, 1953.

16. Milne, W. E., Numerical Calculus, Princeton University Press, Princeton, N. J., 1949.

APPENDIX I

LUBRICANT SPECIFICATIONS

The lubricant used for this investigation was Military Symbol 2110TH obtained from the U. S. Navy Marine Engineering Laboratory, Annapolis, Maryland. This lubricant had a relatively lower optical absorption of light than did the other five lubricants obtained from Annapolis. Below are listed the specifications supplied with the lubricant

Pour Point, degrees F, maximum	-10
Flash Point, degrees F, minimum	325
Water	None
Kinematic Viscosity, Centistokes	
At 0 degrees F, maximum	2400
At 210 degrees F,	5.3 - 6.7

Assuming a linear variation of viscosity with temperature, the above data for kinematic viscosity was plotted and is shown in Figure A-1. Figure A-2 shows the variation of viscosity with pressure. This data was obtained from the ASME Pressure-Viscosity Report [15] using sample 29-F. This sample has nearly the same viscosity as 2110TH and can be used to show the pressure-viscosity relationship of 2110TH.

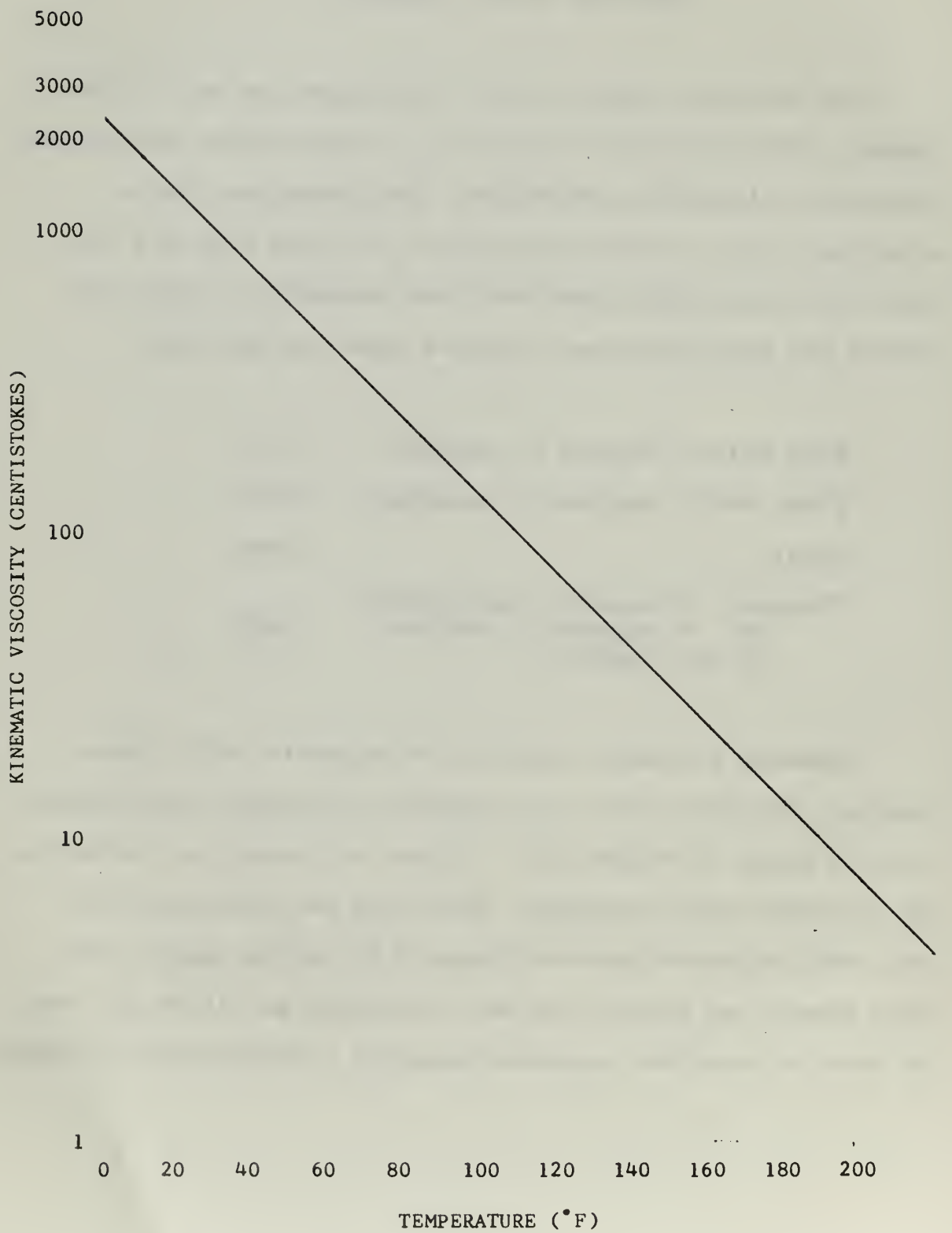

FIGURE A-1. VISCOSITY vs TEMPERATURE FOR 2110TH OIL

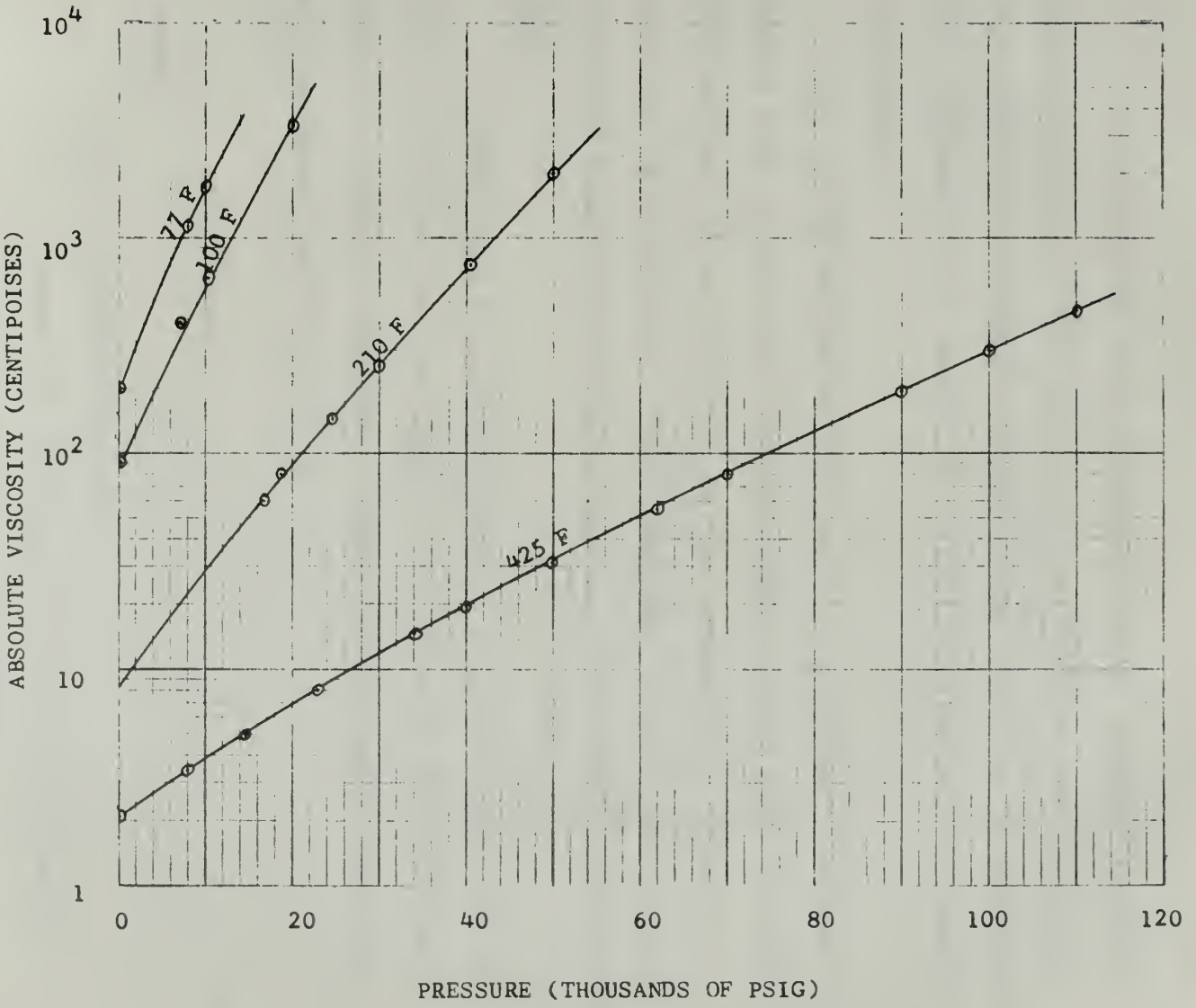

FIGURE A-2. VISCOSITY vs PRESSURE FOR 2110TH OIL

APPENDIX II

CORRELATION OF LOAD AND DROP ANGLE

In any type of tests conducted under dynamic loading conditions, one of the difficulties encountered is obtaining data on the pressure to which the oil film is subjected. This information is useful in relating experimental results to theory.

One of the unique advantages of a continuous measuring system such as the light system used in this work is that information can be obtained on the pressure to which the oil film is subjected. This advantage is lost when a short duration measuring technique such as the x-ray technique is used.

In obtaining oil film pressure, the first step is to obtain the equation for angular momentum of the pendulum about its axis of rotation. Since this is pure rotation, angular momentum reduces to:

$$H_o = I_o \omega \qquad (1)$$

where

H_o = angular momentum

I_o = moment of inertia about axis of rotation

ω = angular velocity of rotation

Since angular momentum equals the moment of linear momentum, one can obtain:

$$H_o = h_o r \qquad (2)$$

where r is the distance from the point of rotation to the point of interest. For pure rotation of the pendulum about its axis of rotation, it can be shown that the linear momentum vector passes through the center of percussion. Since the pendulum was designed so that the center of percussion and point of impact of the two test surfaces coincide, r is the distance from the axis of rotation of the pendulum to the axis of the disk.

Knowing that angular velocity is related to linear velocity by:

$$\omega = v/r \tag{3}$$

one can substitute from Equations (1) and (3) into Equation (2) and obtain:

$$h_o = I_o v/r^2 \tag{4}$$

where

$I_o = 2.09$ inch-lb-sec^2 (determined experimentally)

$r = 12.00$ inches

Using these values, Equation (4) reduces to:

$$h_o = 0.0145\ v \text{ lb-sec} \tag{5}$$

The relationship between linear momentum and linear impulse is:

$$\Delta h_o = \int_{t_1}^{t_2} F\ dt \tag{6}$$

and by substitution from Equation (5):

$$\int_{t_1}^{t_2} F\ dt = 0.0145\ \Delta v \tag{7}$$

Equation (7) may be simplified by the approximation:

$$\sum_{o}^{n} F\ \Delta t = 0.0145\ \Delta v \tag{8}$$

Solution of this equation may be obtained by numerical differentiation. For example, selecting a time interval of three, the following formula from Milne [16] may be used:

$$F = 1/6h \left[-2y_o + 9y_1 - 18y_2 + 11y_3 \right] \qquad (9)$$

where

h = time interval selected

$y_o = 0.0145\ v_o$

$y_1 = 0.0145\ v_1$

$y_2 = 0.0145\ v_2$

$y_3 = 0.0145\ v_3$

The advantage of a continuous measuring technique now becomes clear. Knowing the velocity of approach of the two test surfaces which, in the case of the light system can be obtained from the photographic trace, the force can be obtained. Selection of the number of points and the time interval in the solution by numerical differentiation will depend upon the results of each individual test.

Knowing the force of impact, the pressure in the thinly squeezed oil film is obtained by:

$$P = F/A \qquad (10)$$

where

A = Hertzian contact area

$$A = w \times b \qquad (11)$$

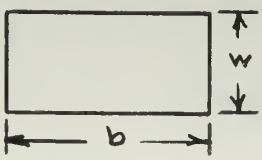

where b is the face width of the test surfaces and w is defined by:

$$w = \frac{2S_{cmax}}{1/r_1 + 1/r_2} \left[\frac{1 - \nu_1^2}{E_1} + \frac{1 - \nu_2^2}{E_2} \right] \qquad (12)$$

where

S_{cmax} = maximum Hertzian stress

ν = Poisson's ratio

E = Young's modulus

r_1, r_2 = radii of cylinders in contact

Assuming $\nu_1 = \nu_2 = 0.3$ and $E_1 = E_2 = 3.0 \times 10^7$ psi and using values of $r_1 = 2.0$ inches and $r_2 = 3.0$ inches, Equation (12) reduces to:

$$w = 1.458 \times 10^{-7} S_{cmax} \qquad (13)$$

Now, by again assuming Poisson's ratio = 0.3, the formula for S_{cmax} reduces to:

$$S_{cmax} = \left[\frac{0.35 F (1/r_1 + 1/r_2)}{b (1/E_1 + 1/E_2)} \right]^{1/2} \qquad (14)$$

Substituting values into Equation (14) it reduces to:

$$S_{cmax} = 2.96 \times 10^3 (F)^{\frac{1}{2}} \qquad (15)$$

Combining Equations (15) and (13) and substituting the result into Equation (11), we have:

$$A = 2.15 \times 10^{-4} (F)^{\frac{1}{2}} \qquad (16)$$

Substituting Equation (16) into Equation (10), the final equation for pressure in the thinly squeezed oil film is then:

$$P = 4640 (F)^{\frac{1}{2}} \qquad (17)$$

Equation (17) shows that oil films under dynamic loading can be subjected to very high pressures. Future investigation of thin oil films using an x-ray technique should attempt to relate the rate of change of count rate to pressure by the method shown above.

APPENDIX III

ABSORPTION DATA ON TEST SURFACES

Little information is available on the absorption of x-rays in 2110TH lubricants. This absorption effect was relatively simple to obtain, however, and is shown in Figure 18 . These calibration curves for air and then for lubricant between the test surfaces, shows the effect of 2110TH on the copper x-ray spectrum used.

Since a relatively thick x-ray beam was used, some of the x-ray beam will fall upon the steel test surfaces. It is therefore important to know the absorption data of the steel disks used in squeezing the lubricant. In considering absorption data, there are several absorption coefficients which are of interest. Two in particular are the mass absorption coefficient, μ , and the linear absorption coefficient, μ_l , which are related by;

$$\mu = \mu_l / \rho \tag{1}$$

where

ρ = density in grams per cubic centimeter

Most tabulated data on the absorption of x-rays by substances is given in terms of the mass absorption coefficient. Since x-ray absorption is an atomic property, the mass absorption coefficient for any material is the sum of the weight fractions of the mass absorption coefficients of the elements present:

$$\mu = W_A \mu_A + W_B \mu_B + \ldots\ldots \tag{2}$$

This equation is always considered valid for monochromatic x-rays and is usually valid for work with polychromatic x-rays.

The linear absorption coefficient becomes important in determining intensities. The linear absorption coefficient is given by:

$$\ln \left[I_1/I_2\right] = \mu_\ell X \qquad (3)$$

Where x is the thickness of the irradiated sample. Thus, by knowing the linear absorption coefficient of the material for x-rays of different wavelengths, one may observe the absorption effect of the material. In this work the two disks which were used to obtain the thinly squeezed oil films were AlSl 8620. The approximate composition and density of this steel is shown below:

	C	Mn	Ni	Cr	Mo	Fe
W%	0.2%	0.8%	0.5%	0.5%	0.2%	97.8%
$\rho\left(\frac{gms}{cm^3}\right)$	1.60	7.20	8.90	7.10	10.2	7.86

The overall density of this steel based on the weight fractions of elements as listed above is 7.848 grams per cubic centimeter.

Using the data tabulated in Liebhafsky, et. al., [13] and Equations (1) and (2), the following absorption data can be tabulated. The wavelength, λ , is in angstroms, the mass absorption coefficient is in units of centimeters squared per gram and the linear absorption coefficient is

in units of centimeters^{-1}.

λ	μ	μ_ρ
0.1	.26558	2.084
0.15	.58156	4.564
0.2	1.1639	9.134
0.25	2.0252	15.894
0.3	3.454	27.107
0.4	7.625	59.842
0.5	14.136	110.94
0.6	23.776	186.59
0.7	35.859	281.42
0.8	52.970	415.72
0.9	73.651	578.03
1.0	99.630	781.92
1.5	308.95	2424.7
2.0	82.364	646.41
2.5	162.45	1274.94
3.0	255.16	2002.5
4.0	510.59	4007.2
5.0	877.1	6883.6
6.0	1394	10940
7.0	2038	15995

By relating this tabulated data to Figure 7 , showing the copper spectrum, one can observe that a very negligible portion of the x-ray beam will pass through the steel disks. This agrees with the findings of Sibley and Orcutt who

concluded that radiation passing through the steel disks they were using contributed less than one millionth of an inch to film thickness measurements. The slight decrease in absorption coefficients between 1.5 and 2.0 angstroms is due to the K absorption edges. This is a phenomena whereby for any given element, the absorption coefficient undergoes a marked decrease for a slight increase in wavelength.

INITIAL DISTRIBUTION LIST

		No. Copies
1.	Defense Documentation Center Cameron Station Alexandria, Virginia 22314	20
2.	Library U. S. Naval Postgraduate School Monterey, California	2
3.	Commander, Naval Ship Systems Command Department of the Navy Washington, D. C. 20360	1
4.	Professor E. K. Gatcombe Department of Mechanical Engineering U. S. Naval Postgraduate School Monterey, California	1
5.	LT Robert L. Towle, USN 1 Beverly Court Belleville, New Jersey	1
6.	Department of Mechanical Engineering U. S. Naval Postgraduate School Monterey, California	1

DOCUMENT CONTROL DATA - R&D

(Security classification of title, body of abstract and indexing annotation must be entered when the overall report is classified)

1. ORIGINATING ACTIVITY (Corporate author)	2a. REPORT SECURITY CLASSIFICATION
Naval Postgraduate School Monterey, California	UNCLASSIFIED
	2b. GROUP

3. REPORT TITLE

The Measurement of Thin Oil Films Under Dynamic Loading Conditions Using Light and X-ray Techniques

4. DESCRIPTIVE NOTES (Type of report and inclusive dates)

Thesis

5. AUTHOR(S) (Last name, first name, initial)

TOWLE, Robert L., LT, USN

6. REPORT DATE	7a. TOTAL NO. OF PAGES	7b. NO. OF REFS
June 1967	89	16

8a. CONTRACT OR GRANT NO.	9a. ORIGINATOR'S REPORT NUMBER(S)
N. A.	N. A.
b. PROJECT NO. N. A.	
c.	9b. OTHER REPORT NO(S) (Any other numbers that may be assigned this report)
d.	N. A.

10. AVAILABILITY/LIMITATION NOTICES

[redacted]

11. SUPPLEMENTARY NOTES	12. SPONSORING MILITARY ACTIVITY
N. A.	Naval Postgraduate School Monterey, California

13. ABSTRACT

This work attempted to study the behavior of thin oil films under dynamic loading conditions using light and x-ray techniques. This was done by passing light and x-ray beams between two cylindrical disks which suddenly squeezed oil films between them. The light technique presents a time variation of oil film thickness under sudden load conditions with good results. The x-ray technique attempted to measure counts from the x-ray beam during the very short time interval of minimum film thickness. Erratic and unreliable results from use of this technique indicate a different approach will have to be taken to measure thin oil films under dynamic loads.

DD FORM 1 JAN 64 1473

14 KEY WORDS	LINK A		LINK B		LINK C	
	ROLE	WT	ROLE	WT	ROLE	WT
Oil film thickness						
X-ray measurement						
Light measurement						

thesT764
DUDLEY KNOX LIBRARY
3 2768 00416378 2
DUDLEY KNOX LIBRARY